energy&fuels

pubs.acs.org/EF Review

Recent Advances in Carbon Dioxide Sequestration in Deep Unmineable Coal Seams Using CO_2-ECBM Technology: Experimental Studies, Simulation, and Field Applications

Grant Charles Mwakipunda, Yuting Wang, Melckzedeck Michael Mgimba, Mbega Ramadhani Ngata, Jeremiah Alhassan, Christopher N. Mkono, and Long Yu*

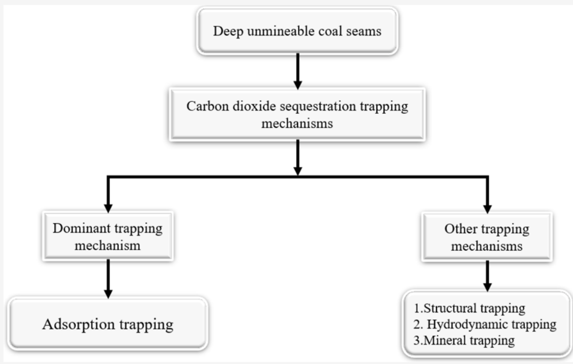

ABSTRACT: CO_2-enhanced coalbed methane (CO_2-ECBM) technology helps to store CO_2 while producing a clean source of energy (CH_4) through the sorption process. This technique can sequester much CO_2 at low temperatures and pressures while recovering CH_4, which will help offset the associated costs, such as capturing injection gases, drilling and completion infrastructure, compression, and injection expenses. This review paper critically analyzes the CO_2 sequestration potentiality in deep unmineable coal seams. The results revealed that, despite several researchers' insights from proposed concepts, experimental data, modeling and simulations, and pilot tests, there are no reported full field CO_2-ECBM technology applications for CO_2 sequestration and CH_4 recovery because implementing the projects is uneconomical. Also, CO_2 sequestration and CH_4 recovery effectiveness on coal seams depend on wettability changes of the CO_2−H_2O−coal system. The identified research gaps and challenges in this paper are going to help various researchers and shareholders in conducting extra investigations toward full field application of CO_2 sequestration while simultaneously producing a clean source of energy (CH_4) in deep unmineable coal seams to meet the Paris climate summit agreement to achieve net zero emissions by 2050 and a maximum global temperature rise of 1.5 °C.

1. INTRODUCTION

In recent years, emissions of greenhouse gases (GHGs) in the atmosphere have increased. In 1990, total GHG emission was 37.86 billion tonnes, in 2000 was 41.34 billion tonnes, in 2010 was 50.27 billion tonnes, in 2020 was 52.59 billion tonnes, and in 2021 was 54.59 billion tonnes.[1−4] This rapid increase in emissions has caused a global climatic change. However, global total GHG emissions decreased by 4.7% during the COVID-19 pandemic from 2019 to 2020. According to the United Nations environmental program (UNEP) report in 2022, the G20 countries contribute 75% of GHG emission into the atmosphere. The top six emitters of GHGs in the World are China, 13.71 billion tonnes; the United States, 5.93 billion tonnes; India, 3.9 billion tonnes; Russia, 2.41 billion tonnes; Brazil, 2.15 billion tonnes; and Indonesia, 2.05 billion tonnes. Africa is the least emissive continent of GHG emissions. Currently, for major GHG emitter countries worldwide, especially China and the U.S., their main energy source is coal, which releases large amounts of carbon gases after burning.[5] China only releases over 27.3% of global GHGs, while the U.S. releases almost half of that of China. Global unmineable coal seam gas reserves are approximately 256 trillion m^3.[6]

Among GHGs, CO_2 is the most emitted GHG in the atmosphere, accounting for 74.4% of the pollutants, as shown in Figure 1. In 1950, the world emitted 6 billion tonnes and in 1990 reached more than 22 billion tonnes. Currently, there is an average of 50 billion tonnes of carbon emission per year.[1,7,8] According to the global summit held in Glasgow, Scotland in 2021, which reviewed the five-year Paris summit agreement implementation of reaching a maximum global temperature increase of 1.5 °C, to achieve the global goal there is a need to cut 45% of current emissions by strengthening and implementing the agreed upon policies. The current policies lead to an increase of 2.8 °C and may be 2.6 °C by 2100.[9] However, if implemented effectively, carbon capture, utilization, and storage (CCUS) can help achieve the Paris climate summit agreement to achieve net zero emissions by 2050 and a maximum global temperature rise

Received: August 9, 2023
Revised: September 29, 2023

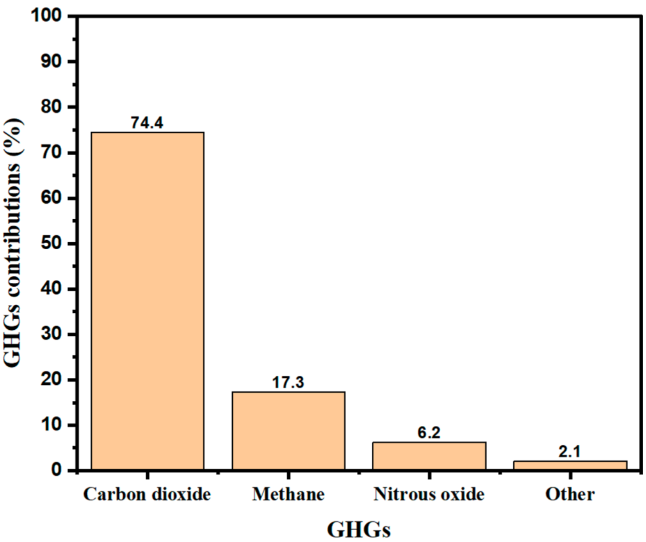

Figure 1. GHG contributions to air pollution. Data retrieved from ref 1.

of 1.5 °C.[10−14] It involves capturing, transporting, and storing it underground or utilizing it for industrial purposes.[15,16] There are many ways of sequestrating CO_2 in geological formations, as discussed by ref 17. Nevertheless, storage of CO_2 in deep unmineable coal seams is not given much attention or implemented. Permanent CO_2 sequestration in deep unmineable coal seams is still under research. Globally, unmineable coal seems to have the potential of sequestrating approximately 3−350 gigatonnes of CO_2 while producing a clean source of energy of more than 150% of CH_4 through CO_2-enhanced coal bed methane (CO_2-ECBM) technology if utilized properly.[18] Among the factors affecting CO_2-ECBM technology applications are the following: permeability reduction, swelling or shrinkage of the matrix, and competitive adsorption and sorption capacity.[19]

In 1972,[20] for the first time, the concept of recovering CH_4 from crushed coal samples by injecting CO_2 was proposed. The development of ECBM can be traced back to the early 1990s when refs 21 and 22 proposed the potentiality of CH_4 recovery and CO_2 sequestration by injecting CO_2/N_2 in deep unmineable coal seams by a depressurization technique. The first ECBM field pilot test was conducted in Tiffany and Allison units of San Juan Basin, New Mexico, USA, in 1995. The pilot test was successful but faced challenges such as permeability reduction and an abrupt rise of pressure near the injection well due to CO_2 adsorption in the coal surface after swelling and shrinkage in the coal seams.[23,24] Hitherto, many successful laboratory experiments, simulations, and pilot tests have been conducted in some coal reservoirs utilizing CO_2-ECBM technology. This has brought substantial attention to researchers to probe CO_2/CH_4 dynamic interaction effects and CH_4 recovery mechanisms with the feasibility of sequestrating CO_2 in deep unmineable coal seams.[25−31]

Even though CO_2-ECBM technology has been tested successfully in different areas to recover CH_4 and for CO_2 sequestration, most are uneconomical.[32−34] Hitherto, there are still fundamental principles of this technology that need to be examined to understand the underlying processes of enhancing production and sequestrating CO_2 to make the technology economical. There are several recently published review papers on enhancing CH_4 recovery while sequestrating CO_2 in deep unmineable coal seams utilizing CO_2-ECBM technology. However, none of the reviews analyzed and discussed the dynamic interaction between CO_2 and H_2O during staged CO_2-ECBM flooding at in situ reservoirs, which results in wettability change, which is important for CO_2 sequestration. Further, in this Review, nanotechnology application during CO_2 sequestration in shallow CBM reservoirs is discussed. Additionally, this Review uniquely analyzes the unprecedented machine learning application in unmineable coal seams during CO_2-ECBM technology application for CO_2 sequestration prediction purposes. Furthermore, this review paper reports the four possible CO_2 trapping mechanisms in deep unmineable coal seams for the first time. The major sections of this review paper include the following: the introduction, theory, experimental parts, modeling and simulation of CO_2-ECBM, field applications, wettability alteration during CO_2-ECBM application, nanotechnology application during CO_2 sequestration in shallow CBM reservoirs, challenges, research gaps, and perspective of storing CO_2 sequestration in deep unmineable coal seams, and conclusions.

2. RESERVOIR SCREENING CRITERIA FOR CO_2-ECBM TECHNOLOGY APPLICATION

To avoid risk of CO_2 leakage, there are some properties which a CBM reservoir must have. Before application of ECBM technology in the unmineable coal field, the following geological criteria must be met for effective and efficient CO_2 sequestration. These criteria lead to project success as discussed in this section.

The reservoir screening criteria include the following: (1) Reservoir homogeneity: laterally continuous and vertically compartmentalized coal seam reservoir(s) are favorable for ECBM. This keeps the injectant contained within the reservoir and allows for more effective lateral sweeps throughout the reservoir. This shows that homogeneous reservoirs influence CO_2 adsorption and CH_4 desorption from the coal surface which influence coal swelling and shrinkage, respectively, that affect effective stress.[19,35,36] (2) Minimal faulting/folding: folded and faulted reservoirs are undesirable. Closely spaced faults can isolate reservoir blocks, preventing the effective sweep. Faults may deflect the injectant from the reservoir, lowering recovery and sequestration. Structurally difficult locations have damaged coal cleat systems and limited permeability.[35,36] (3) Optimal depth range: similarly to conventional CBM, ECBM tends to be effective and efficient when operated with a depth window that varies according to the basin. ECBM cannot be successful at shallow depths due to low reservoir pressure and gas saturation; in deep reservoirs, the formation permeability is always low. Normal coal seam depth is 300−1500 m for CBM. However, in deep reservoirs, hydraulic fracturing can help to improve permeability, and by sustaining pore pressure CO_2 injection can increase permeability.[35−37] (4) Concentrated coal geometry: coal deposits that are concentrated (few, thick seams and low spacing) are preferred over those that are distributed (many, thin seams). Similarly, "completable" coals that are thick are preferable over "targetable" coals that are thin.[35,36] (5) Adequate permeability: permeability is one of the key factors affecting CH_4 production and injection fluid rate during ECBM technology application. High permeability eases flows during the production and injection period to influence ECBM technology application. The moderate cleat permeability for effective ECBM is 1−5 mD.[35,36]

Also, (6) High gas saturation: for ECBM technology application, the coal reservoir should have high initial gas

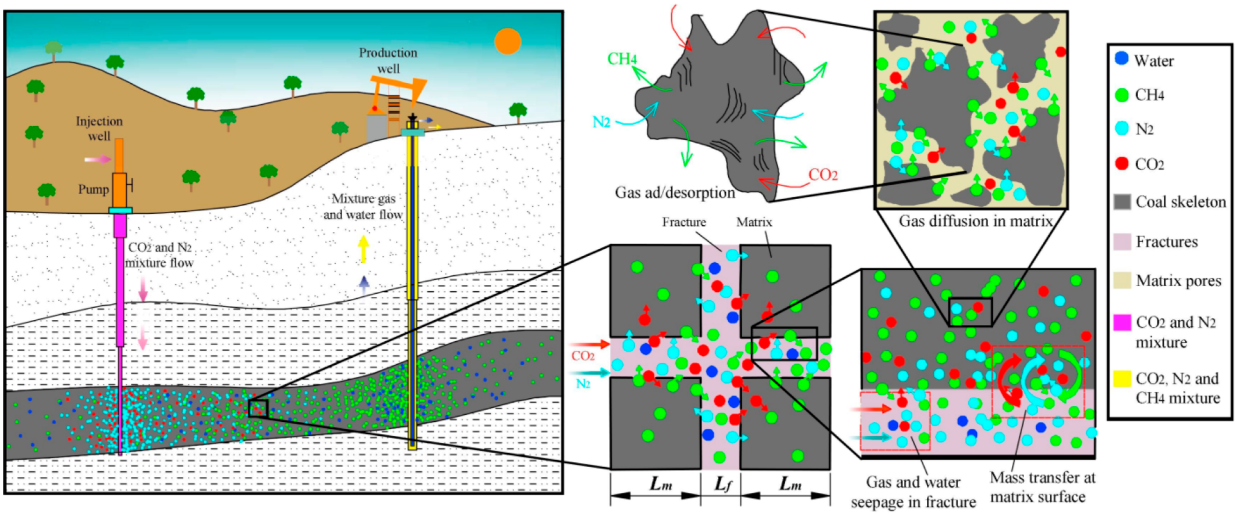

Figure 2. Mass transport in unmineable coal seams during ECBM. This figure was reproduced with permission from ref 68. Copyright 2019 Elsevier.

saturation. For effective ECBM technology, the gas saturation should be high in the range of 90−100% for the sorption process. However, it is revealed that ECBM can work for lower gas saturation (undersaturated), but CH_4 recovery is delayed with high cost.[35,36,38] (7) Optimal coal rank: coal ranks indicate the thermal maturity of the coal, which reflects pressure and temperature deposition history. Coal rank is measured via vitrinite reflectance (R_o). The optimal coal rank is 0.8−1.5% for ECBM technology applications that enhance CH_4 production and CO_2 sequestration.[39,40] Higher amounts of CO_2 can be adsorbed by low-rank coal than by high-rank coal.[35,36,41] (8) Low ash content: coal contains inherent and external mineral matter, termed ash. Ash content is the most influential factor in coal's adsorption capacity.[35,36] Ash infilling primarily clays and carbonates blocks the coal pore system, cleats, and fractures, diminishing gas production.[42] Ref 43 revealed that increasing ash content from 21.24 to 43.47% decreases adsorption capacity, hence resulting in low CO_2 adsorption on the coal surface. In general, low ash concentration improves permeability. (9) High vitrinite content: high vitrinite content increase enhances the CH_4 desorption and CO_2 adsorption capacity of coal, which makes it suitable for ECBM technology application. Coals with vitrinite are well cleated with a high surface specific area and thus are more permeable. Vitrinite affects coal pore structure, especially micropores and pore distribution.[35,36,44,45] (10) High Langmuir volume and pressure are suitable in CO_2-ECBM technology application for CO_2 sequestration and CH_4 recovery.[46]

2.1. Commercial and Technical Criteria for Successful CO_2-ECBM Technology Application. To have successful CO_2 sequestration and CH_4 production in deep unmineable coal seams, there are four commercial and technical criteria to be considered, which are the following: (1) Geology: favorable reservoir conditions such as thickness and coal seam depth at a range of 300−1500 m came across as simple located in simple structural settings and have high in situ permeability greater than 5 mD. (2) Mining: CO_2-ECBM should focus on deep unmineable coal seams where normal mining methods cannot be applied for CO_2 sequestration and CH_4 recovery purposes. (3) CO_2 supplies: CO_2 sources should be continuously supplied at low cost either from anthropogenic sources or reservoirs or captured from power plants. (4) Gas demand: during CO_2-ECBM technology application, CH_4 is produced and CO_2 is sequestrated. However, the technology is expensive, so to offset some of the cost, CH_4 is produced.

3. THEORY

3.1. CO_2 Injection in Coal Seams. Two different ECBM technologies can help to improve CH_4 recovery and CO_2 sequestration. The first option is injecting gas mixtures, mainly CO_2, with inert gas, especially N_2, which helps to reduce methane partial pressure for easy desorption, with CO_2 replacing CH_4 on the coal surface. The effectiveness of CO_2 sequestration and CH_4 recovery depends on the mole fraction ratio of injected gases. The second option involves highly adsorbing gas into the coal seams, especially CO_2, which replaces CH_4 in the coal surface due to its higher affinity to the coal surface than CH_4.[47−50] CO_2 adsorption on the coal surface is faster than CH_4 adsorption, and CH_4 replacement by CO_2 is more rapid than the reverse process.[6] CO_2 and CH_4 interact with molecules on the coal surface, changing adsorption energy, molecular bonds, and equilibrium distance. These gases adsorb on coal surfaces physically, not chemically.[51] CO_2 gas injection into coal cleats reduces the partial pressure of CH_4 in the free gas phase, deprives upsetting the reservoir pressure, and increases the desorption of CH_4 from the coal matrix.[52] However, the main challenge after CO_2 injection in the coal surface is permeability reduction due to its swelling and shrinkage and effective stress changes after the adsorption process, which results in the CH_4 production rate decrease. In addition, the adsorption process results in a decreased CO_2 injection rate because a highly pressurized zone is created by adsorbed CO_2.[24]

Coal, as a mixture of organic and inorganic materials, has several features that influence the sorption process. The coal seam is a dual porosity reservoir system comprised of a matrix with macroporosity and a micro natural fracture system known as the cleat network system.[53] Microscopic pores in coal govern gas adsorption and desorption on the coal matrix surface. They are critical for CBM diffusion (via nanoscale pores) and seepage (via micrometer-to-millimeter holes and fractures).[54] The coal seam's permeability, governed by Darcy's flow, and intrinsic permeability, governed by Fick's diffusion, determine the CO_2 movements in the coal seams. The general gas transport in coal fissures consists of three stages: adsorption/desorption, diffusion in micropores, and transport in cleats. In coal fissures,

https://doi.org/10.1021/acs.energyfuels.3c03004
Energy Fuels XXXX, XXX, XXX−XXX

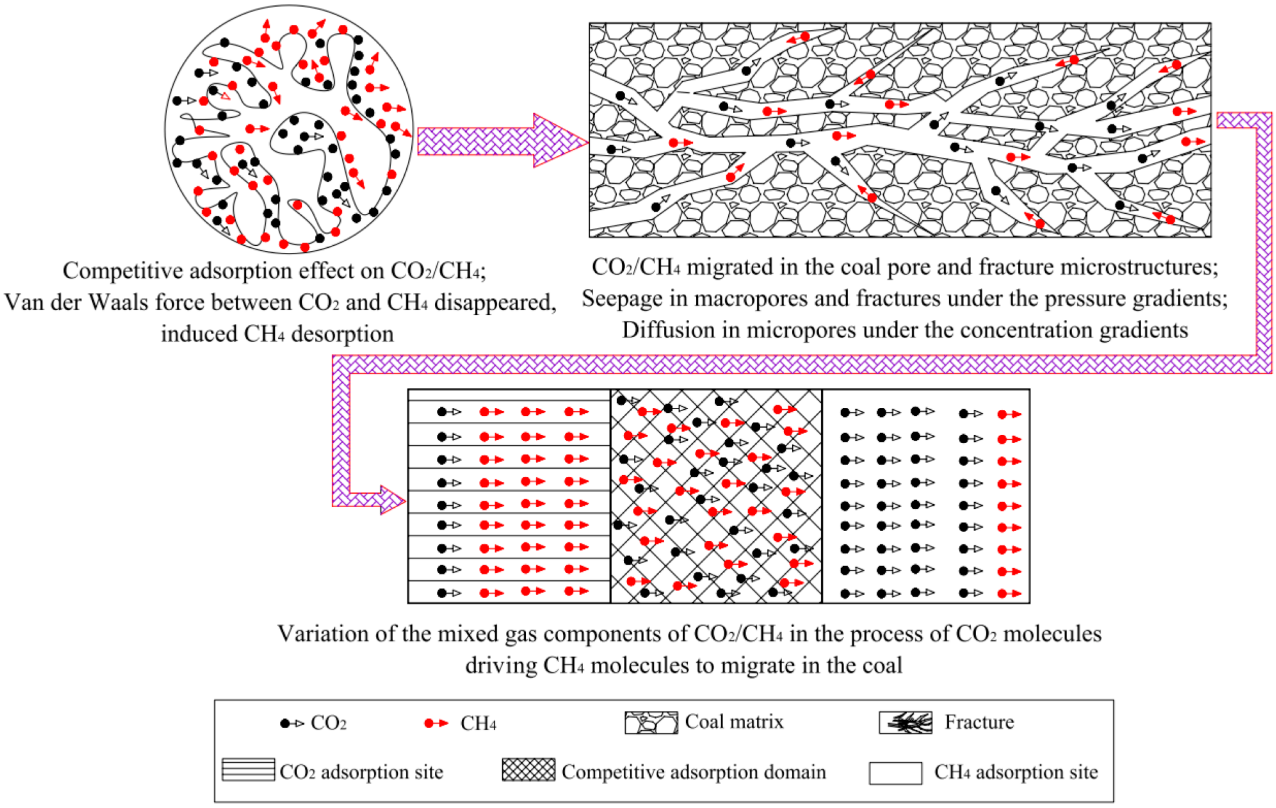

Figure 3. Competitive sorption between CO_2 and CH_4 in coal matrix. This figure was reproduced with permission from ref 86. Copyright 2021 Elsevier.

there is competitive adsorption during the ECBM process, specifically, CO_2 adsorption and CH_4 desorption. Other important coal properties affecting the sorption process include the following: (1) Coal rank: coals are classified based on their rank or thermal maturity. The three primary coals are lignite, bituminous, and anthracite, in order of decreasing coal rank. Coal rank is measured using carbon content, and as carbon content increases, coal rank increases, as discussed by ref 55 that 60−67 db% is lignite coal, 75−80 db% is sub-bituminous coal, 80−90 db% is bituminous coal, and 90−95 db% is anthracite coal. Porosity and permeability decrease as coal rank increases. Medium coal rank (bituminous) has optimal gas content and permeability. Generally, as the coal rank increases, the CO_2 storage capacity increases.[56] (2) Maceral content: high vitrinite reflectance is preferred for ECBM technology application.[57] (3) Moisture content: increasing moist content decreases CO_2 adsorption capacity.[58] In addition to coal characteristics, in situ pressure and temperature affect CO_2 retention capacity.[59] As temperature rises, the coal adsorption capacity decreases. Also, as pressure increases, the adsorption capacity of coal increases.[60]

3.2. CO_2 and CH_4 Transport Mechanisms in Coal Seams. Technical development of CO_2-ECBM technology requires understanding the underlying transport mechanism and gas sorption in coal seams. Understanding these processes on microscopic and macroscopic scales is important in predicting CH_4 production and CO_2 sequestration.[61,62] Coal seams' gases and water transport differ from that in conventional reservoirs. Gases transport mechanisms in coal seams occur on two scales, which are laminar flows and diffusion and sorption flows. Laminar flows occur in coal cleats driven by pressure differences governed by Darcy's flow[63] while diffusion and sorption flows in the coal matrix are restrained by concentration differences governed by Fick's law of diffusion[64] as shown in Figure 2. In the coal matrix is where the CO_2 sequestration occurs after CO_2 and CH_4 sorption processes.[65−67]

3.3. Competitive Sorption between CO_2 and CH_4. Understanding competitive sorption between CO_2 and CH_4 (Figure 3) on the coal surface is crucial for understanding underlying mechanisms during CO_2-ECBM technology application for CO_2 sequestration and CH_4 recovery purposes.[69] Several experiments[70−76] and developed models[55,68,77−81] reported the CO_2−CH_4 sorption process on the coal surface. It has been found that after CO_2 injection into the coal formation, CH_4 adsorption equilibrium is drastically disrupted; thus, the potential reaction between CO_2 and coal and CH_4 occurs, witnessed by changes in coal structure and composition; after that, coal becomes enriched with CO_2. Adsorbed CO_2 excels more than twice that of desorbed CH_4 on the coal surface due to pore structure enlargement (porosity increase) and permeability reduction after the CO_2 swelling process.[82] In a low-pressure environment, CO_2 sorption capacity on the coal surface may reach at least 10 times the sorbed CH_4.[28,83−85] Further, the higher adsorption potential energy of CO_2 compared to CH_4 causes van der Waals forces between the coal matrix and CH_4 to diminish; thus, CO_2 adsorbs easily into the coal surface. Furthermore, the higher molecular freedom of CH_4 compared to CO_2 causes CH_4 to desorb easily from the coal matrix to give space for CO_2 adsorption. This proves that CO_2 replaces CH_4 from the coal surface due to its high affinity to the coal surface compared to CH_4 which is released and flows toward the production wellbore.[86,87]

3.4. CO_2 Sequestration Trapping Mechanisms in Unmineable Coal Seams. Due to their accessibility and

https://doi.org/10.1021/acs.energyfuels.3c03004
Energy Fuels XXXX, XXX, XXX−XXX

cost-effectiveness, deep unmineable coal deposits have been recommended as a permanent and long-term CO_2 storage option. After CO_2 is injected into the coal seams, it replaces CH_4 due to its higher affinity for coal formation than CH_4. Storage potentials, security, and project monitoring depend on reservoir storage capacity and CO_2 trapping mechanism. There are four primary mechanisms in which CO_2 can be stored in the unmineable CBM:[88] (1) adsorption trapping mechanism, (2) stratigraphic or structural trapping mechanism, (3) hydrodynamic (solubility) trapping mechanism, and (4) mineral trapping mechanism. In the adsorption trapping mechanism, CO_2 is adsorbed in the coal surface due to its higher affinity capacity than that of methane, and this is the dominant trapping mechanism, approximately 95−98% of total storage.[41] Nevertheless, after the maximum adsorption capacity is attained, adsorption capacity decreases with increasing depth. In stratigraphic or structural trapping mechanisms, CO_2 is stored as a free phase triggered by the presence of impermeable cap rock due to anticlines or faults that prevent upward movement.[89] In the hydrodynamic trapping mechanism, CO_2 is dissolved in brine and forms carbonic acid, which later decomposes to form carbonates and hydroxyl ions.[90,91] In the mineral trapping mechanism, the dissolved CO_2 in brine forms carbonic acid, which can later precipitate to form minerals after interacting with rock minerals.[92] The mineral trapping mechanism takes thousands of years to form minerals; however, it is believed to be the safest trapping mechanism compared to others.

4. EXPERIMENTS

Many researchers have conducted experiments to probe the potentiality of CO_2-ECBM technology application to CO_2 sequestration toward decarbonization and recovery of clean energy sources. The process involves the injection of CO_2 or CO_2 mixed with other gases in the CBM reservoirs, which adsorb into the coal surface while CH_4 desorbs due to its lower affinity to the coal surface than CO_2; then, most CO_2 is stored through an adsorption mechanism with the least stored through other mechanisms discussed in section 3.4. Hence, this section discusses different findings of conducted experiments showing great success in CO_2 sequestration through CO_2-ECBM technology application.

Reference 26 experimented on the impacts of injecting CO_2 in coalbed methane by observing the CO_2 sequestrated and CH_4 recovered in coal seams. In their experiments, synergistic effects of CO_2 sequestration and CH_4 recovery were considered. A large-scale multifunctional apparatus designed closely to the actual CBM reservoir simulated CO_2-ECBM technology application. The apparatus gave the actual conditions of each reservoir point from injection to production wells. To reflect the reality of the field operation, conventional production was utilized first, followed by the CO_2-ECBM technique at different pressures. The CH_4 recovery efficiency was 66.67% during conventional production, and after CO_2 injection in the coal seams with a range of pressure of 1−1.0 MPa, the production increased from 66.67 to 93.5% and later reduced to 90.86%. For CO_2 sequestration, when pressure increased from 1 to 1.6 MPa, the efficiency decreased from 67.89 to 43.98%, as shown in Figure 4. For efficient CO_2 sequestration and CH_4 recovery, it was suggested that injection pressure variation is important. In general, higher injection pressure is required during the initial production stage but later needs to be reduced when the production starts to decline. These changes in pressure will influence CO_2 sequestration too.

Also, ref 93 probed the impacts of injecting CO_2 in unmineable coal seams on CO_2 sequestration and CH_4 recovery. A highly bituminous coal sample collected from the Tashan coal mine in China was used. The core-flooding experiments were conducted using a triaxial apparatus under constant high-temperature and -pressure conditions of 37 °C and 12 MPa, respectively, with coal seams buried around 500−600 m as the necessary condition for CO_2-ECBM technology application. The process involved injecting CO_2 at constant pressure in CH_4-saturated coal samples to observe the CO_2 sequestration and CH_4 recovery. The CO_2 was injected five times with a range of injection pressure of 6−10 MPa. The CO_2 sequestration capacity and CH_4 recovery efficiencies are shown in Table 1. Further, high CO_2 injection pressure (9 and 10 MPa) results in faster and higher CH_4 production and greater CO_2 sequestration, but early CO_2 breakthrough makes CO_2-ECBM technology application uneconomical. In addition, moisture content delays the CO_2−CH_4 exchange process in all coals except high-rank coals, resulting in lower CO_2 sequestration and CH_4 recovery.

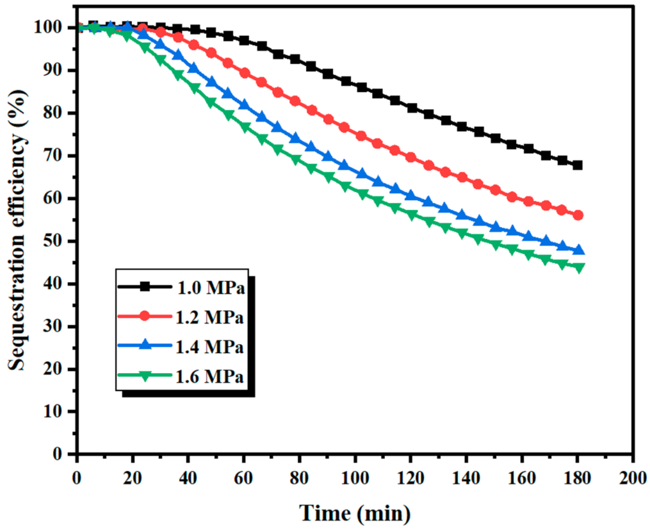

Figure 4. CO_2 sequestration efficiency in different injection pressures. This figure was reproduced with permission from ref 26. Copyright 2023 Elsevier.

Table 1. CO_2 Storage Capacity and CH_4 Recovery Efficiency[a]

CO_2 injection pressure (MPa)	initial CH_4 content (m^3/tonnes)	CH_4 content after CO_2-ECBM application (m^3/tonnes)	CH_4 recovery rate (%)	CO_2 storage capacity (m^3/tonnes)
-	18.53	8.94	51.73	
6	18.51	0.63	96.57	37.25
7	18.37	0.41	97.79	38.02
8	18.46	0.06	99.68	39.88
9	18.46	0	100	40.89
10	18.50	0	100	41.62

[a]Reproduced with permission from ref 93. Copyright 2019 Elsevier.

Further, ref 94 experimented on the consequences of CO_2 injection into a partially filled CH_4 bituminous coal sample collected from San Juan basin coal in New Mexico. The samples were broken into powder during the sorption process to save time during the experiment for an easy diffusion process. Two CO_2 injection sets of experiments were conducted at a pressure range of 300−500 psi. In their investigation, an extended Langmuir (EL) equation was used for predicting adsorbed and desorbed CO_2 and CH_4 recovery during CO_2 injection. In the first experiment, CH_4 adsorption occurred at 1487 psi, followed by sorption at 499 psi with four steps. In this scenario, sorbed CH_4 decreased from 8.6 to 5.0 mL/g. Again, after CO_2 injection at a pressure of 504 psi, the CO_2 sequestrated was 10.3 mL/g while desorbed CH_4 was 2.9 mL/g. In the second experiment, CH_4 adsorption occurred at 1356 psi, followed by sorption at 487 psi with four steps. In this scenario, sorbed CH_4 decreased from 8.2 to 3.7 mL/g. After CO_2 injection at a pressure of 303 psi, the CO_2 sequestrated was 6.8 mL/g, while desorbed CH_4 was 2.9 mL/g. Later, CO_2 was injected at a pressure of 312 psi, in which added

https://doi.org/10.1021/acs.energyfuels.3c03004
Energy Fuels XXXX, XXX, XXX−XXX

CO_2 sequestrated was 4.4 mL/g while additional CH_4 recovery was almost zero. The EL model predicts sorbed carbon dioxide effectively but not methane.

In addition, ref 95 investigated the effectiveness of injecting CO_2 in enhancing CO_2 sequestration and CH_4 recovery in high-rank coals (anthracite) from the South Wales coal field. Competitive sorption between $CO_2/N_2/CH_4$ in the coal surface was investigated in the designed experiment to measure their efficiencies on CO_2 sequestration and CH_4 recovery using ECBM technology. Triaxial core flooding experiments with high-pressure−high-temperature (HPHT) control systems were designed and conducted in which CO_2 and N_2 were injected in different periods at 5 MPa and a temperature of 25 °C. The results revealed that during the N_2-ECBM technology application, more CH_4 was produced, with 93% of injected N_2 recovered, increasing the separation process cost. For the CO_2-ECBM technology application, 63% of the CO_2 injected was recovered. Furthermore, in the CO_2-ECBM experiment, CH_4 recovery was 10 and 2.4 times higher than gas injected and stored. The cumulative CO_2 stored during the experiment is shown in Figure 5.

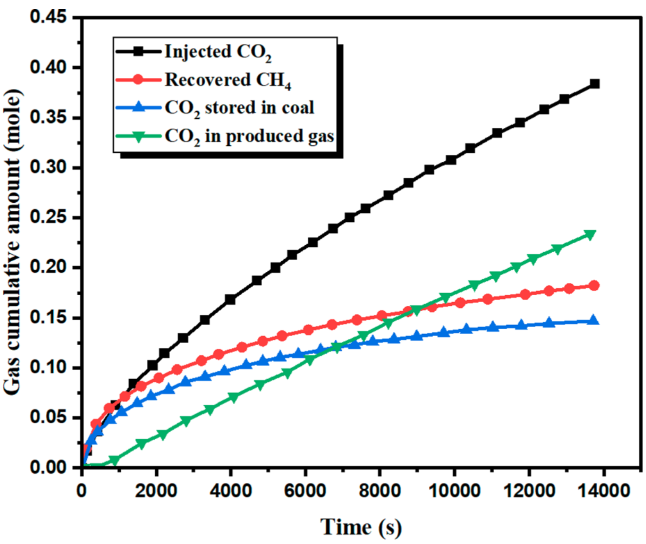

Figure 5. Cumulative CO_2 injected, produced, and sequestrated. This figure was reproduced with permission from ref 95. Copyright 2017 American Chemical Society.

Moreover, ref 96 experimented on the sorption behavior of coal seams in enhancing CH_4 recovery and CO_2 sequestration after CO_2 injection. The experiments were carried out in three different coal seams in which, after being saturated with CH_4, CH_4 desorption by depressurization occurred before CO_2 injection. The coal characteristics used in the experiments are shown in Table 2. It was found that the ability of coal seams to store CO_2 was two to four times in volume compared to that of CH_4, which agreed with previous experiments. The amount of CO_2 adsorbed for different subsequent CO_2 injected is shown in Figure 6. From Figure 6, it is seen that as the injection cycle increases, the coal adsorption capacity increases. Furthermore, CO_2

Table 2. Characteristics of Coal Seams Used in the Experiments[a]

coal seams	moisture content (%)	ash content (%)	temperature condition (°C)	pressure condition (MPa)	CO_2 injection pressure (MPa)
seam 1	10	11.3	45	0.7	3.4
seam 2	8.7	7.8	25	2.8	3.4
seam 3	10	3.9	23.5	5.5	3.7

[a]Reproduced with permission from ref 96. Copyright 2008 Elsevier.

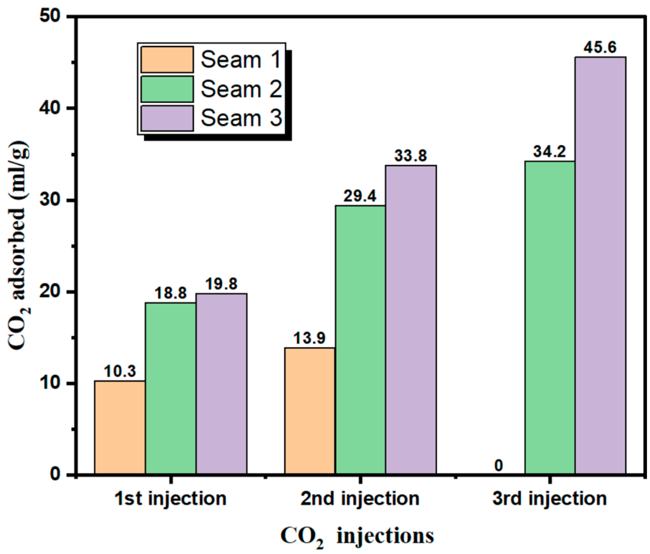

Figure 6. CO_2 adsorbed in different coal seams. This figure was reproduced with permission from ref 96. Copyright 2008 Elsevier.

high affinity is more noticeable in coal seams 2 and 3 than in coal seam 1 due to low ash content, as shown in Table 4. Due to the greater affinity of CO_2 for coal seams than CH_4, all coal seams appeared to be excellent candidates for CH_4 recovery and CO_2 sequestration in all experiments.

Furthermore, ref 97 experimented on the CO_2 sequestration in deep unmineable coal seams in the southern Qinshui Basin in China by injecting Sc-CO_2. In their experiments, different coal samples, namely CZ (bituminous coal) and YW and SH (anthracite coals) from the Shanxi Formation were used to observe the amount of CO_2 adsorbed, CO_2 in the free state, and CO_2 dissolved in free water under different temperature and pressure conditions after Sc-CO_2. The Dubinin−Radushkevich (D−R) model was utilized for fitting Sc-CO_2 adsorption data. The results revealed that most of the injected Sc-CO_2 was adsorbed and free gas capacity should not be neglected, whereas CO_2 dissolved in water was neglected. After calculating the total CO_2 storage capacity of Qinshui Basin, the potential depth for storing CO_2 was 1100−1200 m due to its high porosity and permeability.

Besides that, ref 98 experimented on the CO_2 sequestration in deep coal seams using an HPHT reactor enriched with CO_2-saturated brine and coal samples, namely S1, S2, and S3, collected from the Collie Basin in the western part of Australia. They needed to analyze the interaction effects of CO_2−brine on the coal structure. The experiments were conducted under similar reservoir temperature and pressure conditions of 50 °C and 20 MPa, respectively. The CO_2 was mixed with deionized water with a salt concentration of 5 wt % NaCl to form CO_2-saturated brine injected into deep coal seams. The results revealed that after injected CO_2 interacts with brine, it greatly affects the coal microstructure, which causes mineral dissolution at cleat edges, thus increasing its volume. The CO_2−brine interactions also increase the cleats connectivity, as confirmed in this experiment which increased from 25 to 72.4%. This shows that the space for CO_2 storage increased with its coal permeability for easy injection. It was concluded that when injected CO_2 interacts with brine, it changes the microstructure of coal, which needs to be measured on a microscale to quantify it to improve and predict the storage capacity of coal seams. A summary of different experimental studies on CO_2-ECBM technology application to CO_2 sequestration and CH_4 recovery is shown in Table 3.

5. MODELING AND SIMULATIONS

A simulation study is one of the essential stages which, if implemented successfully, gives the actual feasibility for predicting the future outlook of the intended operation once implemented in the actual field. Several researchers have conducted modeling and simulation studies on the CO_2-

Table 3. Summary of Some Experiments on CO_2-ECBM Technology Applications

references	objectives	experimental conditions	key findings
26	Evaluate CO_2 sequestration efficiency and CH_4 recovery in coal seams through CO_2 injection.	injection pressure of 1−1.6 MPa	CO_2 sequestration efficiency decreased (67.89−43.98%) at higher injection pressure, while the CH_4 recovery increased from 66.67 to 93.5%.
		temperature of −6 to 12 °C	
93	Effects of CO_2 injection in CH_4 recovery and CO_2 sequestration.	injection pressure of 6−10 MPa	Higher injection pressure increased CO_2 sequestration.
		temperature of 37 °C	CH_4 production increased from 51.73% to over 90% at higher injection pressure (>8 MPa).
			High coal rank are favorites for CH_4 production and CO_2 sequestration compared to low-rank coal.
25	Investigate the CH_4 recovery rate and CO_2 sequestration in coal with high water saturation.	injection pressure of 49.4−99.7 MPa	A significant amount of CO_2 adsorbed in the coal surface during cyclic injection.
			Desorption rate plays a significant role in CH_4 production from coal seams.
			CH_4 recovery and CO_2 sequestration increased at high injection pressure and large number of injection cycle.
99	Examine the effects of CO_2 injection pressure on CH_4 replacement and CO_2 sequestration.	injection pressure of 0.6−10 MPa	CH_4 desorption rate increased from 90.2 to 97.8 L.
		temperature of 30 °C	CO_2 sequestration increased from 269.2 to 322.8 L.
96	Investigate the CH_4 recovery after CO_2 injection.	injection pressure of 3.4−3.7 MPa	Coal samples store 2−4 times the amount of CO_2 compared to displaced CH_4.
			CH_4 recovery increased from 40 to 80%.
94	CO_2 injection effects on CH_4 desorption and CO_2 adsorption.	injection pressure of 2.07−3.45 MPa	Extended Langmuir model can predict CO_2 sequestrated not CH_4 recovered.
			Higher injection pressure has more effects on CO_2 stored than on CH_4 recovery.
95	Investigate the effects of injecting CO_2 and N_2 in CO_2 sequestration and CH_4 recovery.	injection pressure of 5 MPa	More CH_4 is recovered during N_2 injection with 94% of it reproduced, which increases separation cost.
		temperature of 5 °C	37% of injected CO_2 was sequestrated during CO_2 injection with low CH_4 recovered compared to N_2 injection.

Table 4. Characteristics of Most Common Simulators for ECBM

	simulators					
characteristics	COMSOL	GEM	ECLIPSE	COMET3	SIMED II	GCOMP
multicomponent gas	√	√	×	√	√	√
dual porosity	√	√	√	√	√	×
mixed gas diffusion	√	√	√	√	√	×
mixed gas adsorption	√	√	×	√	√	√
dynamic permeability and porosity	√	√	√	√	√	√
coal swelling/shrinkage	√	√	×	√	√	√

ECBM technology application toward decarbonization and clean energy recovery. Different analytical models have been developed, and various simulations have been done using established commercial reservoir simulators. Various commercial reservoir simulation software is used to simulate ECBM technology applications, as shown in Table 4. So, this section presents simulation verdicts in two- and three-dimensional models for the CO_2-ECBM technology application to produce CH_4 and CO_2 sequestration.

5.1. Governing Equations. *5.1.1. For Gas Flows.* The gas flow in CBM includes three processes: adsorption, diffusion, and seepage, which are defined by eq 1 and obey Fick's law. The injection process is assumed to be a single-phase flow because water influence is neglected. Also, the model assumes that coal has a single porosity and permeability of[100−103]

$$\frac{\partial m}{\partial t} + \nabla\cdot(\rho_g \vec{q}_g) = Q_s \tag{1}$$

Here

$$Q_s = \pm\frac{M_g(1-\varphi_f)}{\tau RT}(p_m - p_f) \tag{2}$$

$$\vec{q}_g = -\frac{k}{\mu}\nabla p\cdot Q_s \tag{3}$$

where Q_s represents the gas source supply for mas exchange between fracture and matrix systems, kg/ (m^3·s); k stands for permeability in the coal bed, m^2; $\vec{q}_g$ is the Darcy velocity vector of gas; τ is the gas mass exchange factor between fracture and matrix systems, d; μ is the dynamic gas viscosity, Pa·s; and φ_f is porosity in the fracture.

However, the mass of gas in fracture and matrix systems is defined as[100−103]

$$m_m = \rho_g\varphi_m + (1-\varphi_m)\rho_{ga}\rho_c V_{cg} \tag{4}$$

$$m_f = \rho_g\varphi_f \tag{5}$$

$$V_{cg} = \frac{V_L p_m}{P_L + p_m}\exp\left[-\frac{d_2}{1+d_1 p_m}(T - T_t)\right] \tag{6}$$

$$\rho_g = \frac{M_g p}{RT} \tag{7}$$

https://doi.org/10.1021/acs.energyfuels.3c03004
Energy Fuels XXXX, XXX, XXX−XXX

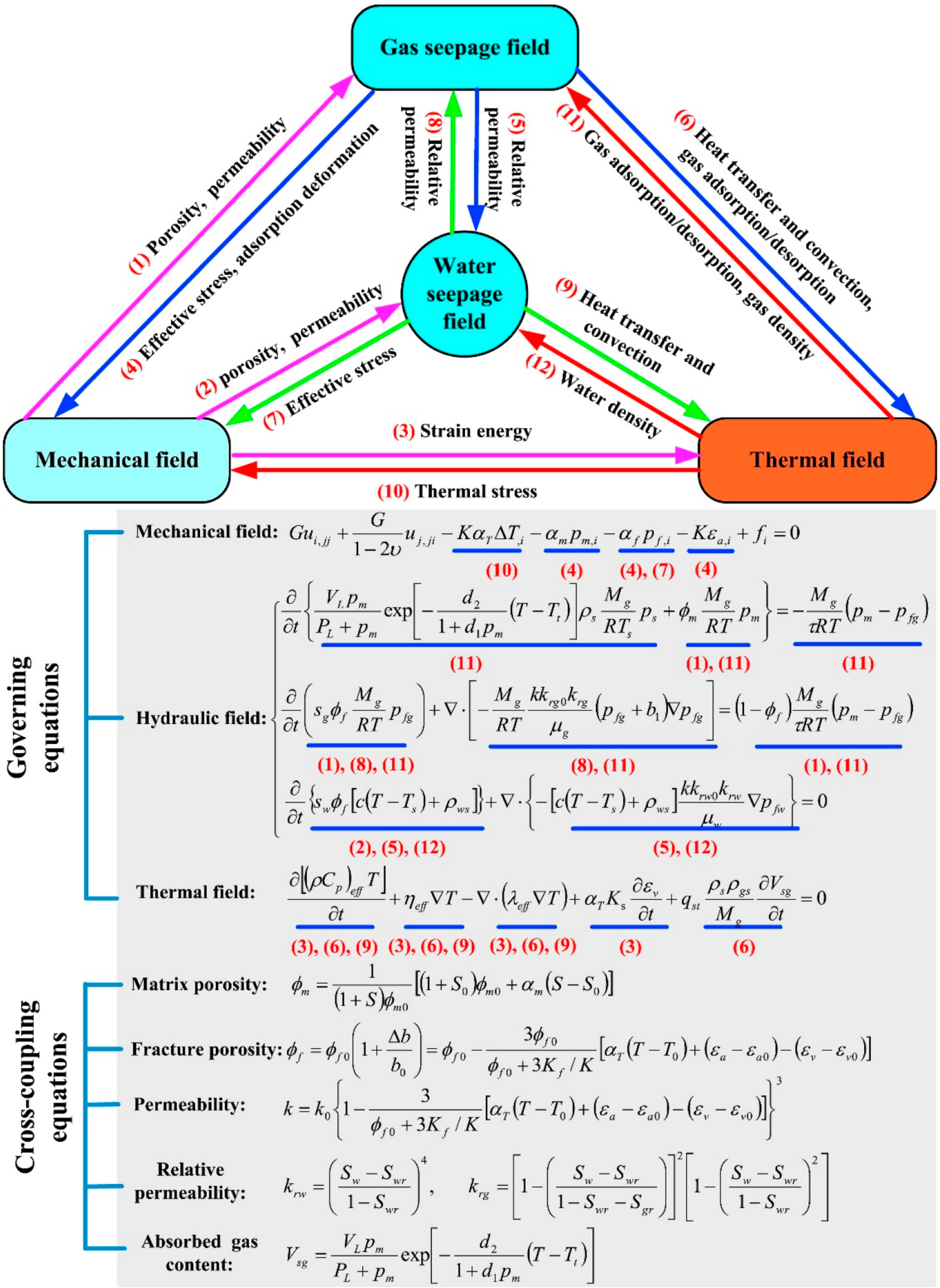

Figure 7. Hydraulic−mechanical−thermal-coupled model, governing equations, and cross-coupling equations for CO_2 sequestration and CH_4 production. This figure was reproduced with permission from ref 110. Copyright 2016 Elsevier.

where ρ_g represents CO_2 density in coalbeds under various reservoir conditions, kg/m^3; R represents the universal gas constant, J/mol·K; M_g stands for gas molecular mass, g/mol; p is pressure in the coal bed, Pa; T is temperature, K ; ρ_{ga} is the density of gas under standard conditions, kg/m^3; ρ_c is the density of the skeleton of coal; subscripts m and f represent matrix and fracture of the coal system; P_L represents Langmuir pressure constant, Pa; V_L represents the Langmuir volume constant, m^3/kg ; V_{cg} stands for adsorbed gas per unit mass of coal skeleton, m^3/kg; T_t is the reference temperature during adsorption, K; and d_1 is the Langmuir pressure factor, kg/m^3.

By substituting eqs 2−7 into eq 4, the mass transport gas equation in the coal fracture and matrix system is obtained:[100−103]

$$\frac{\partial}{\partial t}\left\{\frac{M_g p_m}{RT}\varphi_m + (1-\varphi_m)\rho_{ga}\rho_c V_{cg}\right\} + \nabla\left(-\frac{M_g p_m k_m}{RT\mu}\cdot\nabla p_m\right) = \frac{M_g(1-\varphi_f)}{\tau RT}(p_m - p_f) \tag{8}$$

which is simplified into

Table 5. Comparison of Different Coupling Models for Gas Injection

model types[a]	key factors: coal deformation	matrix fracture mass exchange	heat transfer and nonisothermal adsorption	competitive sorption	water	dynamic diffusion	diffusion	desorption heat	heat rupture	references
GM	√	√				√	√			111
HM	√				√					112
GMT	√		√							113
GMT	√		√	√			√	√		114
GMT	√		√						√	115
THM	√	√	√	√	√		√	√		116
THM	√	√	√		√		√	√		110
THM	√	√	√	√	√	√	√	√		117

[a]HM: Hydromechanical; GMT: thermal-gas-mechanical; THM: thermo-hydro-mechanical; GM: gas-mechanical.

$$\frac{\partial}{\partial t}\left(\frac{M_g p_f}{RT}\varphi_f\right) + \nabla\cdot\left(-\frac{M_g p_f k_f}{RT\mu}\cdot\nabla p_f\right) = -\frac{M_g(1-\varphi_f)}{\tau RT}(p_m - p_f) \tag{9}$$

5.1.2. For Coal Deformation. The Navier−Stokes equation is used to describe the space balance in coal by neglecting inertia force effects, as shown in eq 10.[100,101,103−105]

$$\sigma_{ij} + F_i = 0 \tag{10}$$

where σ_{ij} represents strain tensor components, Pa; and F_i stands for force component, N.

Then the geometric equation explaining the displacement and strain components of coal is expressed as

$$\varepsilon_{ij,j} = \frac{1}{2}(u_{ij} + u_{ji}) \tag{11}$$

where $\varepsilon_{ij,\,j}$ is the strain tensor component, m; and u_{ij} is the displacement component, m.

Since pressure and temperature changes and CO_2 adsorption occur in coal, the coal is subject to stress, resulting in a strain that can be derived from Hooke's law. Then the stress−strain relationship in coal is given as[100,101,103−105]

$$\varepsilon_{ij} = \frac{1}{2G}\sigma_{ij} - \left(\frac{1}{6G} - \frac{1}{9K}\right)\sigma_{kk}\delta_{ij} + \frac{\alpha}{3K}p_m\delta_{ij} + \frac{\beta}{3K}p_f\delta_{ij} + \frac{\alpha_T}{3}(T - T_0)\delta_{ij} + \frac{\varepsilon_s}{3}\delta_{ij} \tag{12}$$

Here $G = \frac{D}{(2+2v)}$, $D = \frac{1}{[1/E_S + 1/(aK_n)]}$, $\alpha = 1 - K/K_s$, $\beta = 1 - K/(aK_n)$, and $\varepsilon_s = \alpha_{sg}V_{cg}$, where K_n is coal fracture stiffness, Pa/m; G stands for the shear modulus stress of coal, Pa; D represents the elastic modulus of coal, Pa; K stands for the bulk modulus of coal, Pa; a is fracture spacing, m; α_{sg} is adsorption strain coefficient, kg/m^3; ε_s is matrix adsorption coal strain; α represents Biot coefficient of the matrix system; E_S represents skeleton Young's modulus, Pa; and α_T stands for thermal expansion coefficient of coal, 1/K.

By combining eqs 10−12, the deformation equation for coal is obtained as shown below:

$$Gu_{i,jj} + \frac{G}{1-2v}u_{j,ji} - \alpha p_{m,i} - \beta p_{f,i} - K\varepsilon_{s,i} - K\alpha_T T_i + F_i = 0 \tag{13}$$

5.1.3. For Thermal Fields. After the injection of CO_2 into the coal seams, the temperature change ensues because of heat exchange between coal and CO_2 and others released from the CO_2 adsorption process. An internal heat source can lower the coalbed temperature field through irregular heat conduction. The governing equation for the thermal field during CO_2 sequestration is determined by applying the law of conservation of energy, as shown in eq 14:[101,103,105−107]

$$\begin{cases} \frac{\partial((\rho C_p)'_c T)}{\partial t} + \eta\nabla T - \nabla\cdot(\lambda_c\nabla T) + K\alpha_T T\frac{\partial\varepsilon_s}{\partial t} + q_{st}\frac{\rho_c\rho_{ga}}{M_g}\frac{\partial V_{cg}}{\partial t} = 0 \\ (\rho C_p)_c = (1 - \varphi_f - \varphi_m)\rho_s C_s + (\varphi_f + \varphi_m)\rho_g C_g \\ \eta = -\frac{k_f}{\mu}\left(1 + \frac{b_1}{p_f}\right)\nabla p_f \rho_g C_g \\ \lambda_c = (1 - \varphi_f - \varphi_m)\lambda_s + (\varphi_f + \varphi_m)\lambda_g \end{cases} \tag{14}$$

where $(\rho C_p)_c$ is the effective specific heat capacity of coal mixed with CO_2, J/m^3·K; C is specific heat capacity, J/m^3·K; η is the convection factor, J/m^2·s; q_{st} is isosteric heat of adsorption, J/mol; subscript g represents CO_2; and λ is thermal conductivity, W/m·K.

5.2. Cross Coupling. The permeability and porosity of the coal seams influence CO_2 sequestration in deep unmineable coal seams. Internal stress and intrinsic coal features influence the dual porosity characteristics of coal seam structure and initial permeability of matrix and fracture systems. When CO_2 is injected, the porosity and permeability of the coal seams change depending on the amount of injected gas and temperature of the coal seams, which are expressed as[100,101,103,105,108,109]

$$\varphi_m = \varphi_{m0} - \frac{\alpha}{K}\cdot\frac{1}{\frac{b_0}{a_0K_f} + \frac{1}{K}}(\alpha_T\Delta T + \Delta\varepsilon_s - \varepsilon_v) \tag{15}$$

$$k_m = k_{m0}\left(1 - \frac{\alpha}{\varphi_{m0}K}\cdot\frac{(\alpha_T\Delta T + \Delta\varepsilon_s - \varepsilon_v)}{b_0/a_0K_f + 1/K}\right)^3 \tag{16}$$

$$\varphi_f = \varphi_{f0} - \frac{3\varphi_{f0}}{\varphi_{f0} + \frac{3K_f}{K}}(\alpha_T\Delta T + \Delta\varepsilon_s - \varepsilon_v) \tag{17}$$

$$k_f = k_{f0}\left(1 - \frac{3}{\varphi_{f0} + 3K_f/K}(\alpha_T\Delta T + \Delta\varepsilon_s - \varepsilon_v)\right)^3 \tag{18}$$

https://doi.org/10.1021/acs.energyfuels.3c03004
Energy Fuels XXXX, XXX, XXX−XXX

where ε_v represent strain volume and subscript 0 represents initial value.

Combining eqs 8, 9, 13, and 14, the hydraulic−mechanical−thermal-coupled model is obtained, as shown in Figure 7. The hydraulic−mechanical−thermal-coupled process in coal seams occurs simultaneously in which pressure, temperature, and stress changes affect each other. The stress field controls gas seepage velocity by controlling coal seam porosity and permeability. In contrast, gas desorption and adsorption change coal skeleton strain, gas seepage velocity affects heat exchange transfer in the coal seam, and temperature strain affects coal seam porosity and permeability. The coupling term relates physical field factors to interact with gas seepage, coal deformation, and thermal equations.[101,103,105] Different established coupling models for gas injection are shown in Table 5.

Reference 118 predicted the storage capacity of the Ishikari coal field by using data collected from laboratory analysis, well logs, and water injection falloff tests. The Ishikari model successfully predicted the amount of CO_2 that can be sequestrated in huff and puff injection and multiwell tests before the pilot test. Simulation analysis revealed that 72% of injected CO_2 during the huff and puff test could be stored in the coalbed during the pilot test, whereas 96% of injected CO_2 could be stored for the multiwell test during the pilot test. It was predicted that 1.2×10^6 tonnes of CO_2 could be sequestrated in the Ishikari coal field. On the other hand, the CH_4 production rate increased from 500 to 1300 m^3/day during CO_2 injection. Also, ref 101 established a numerical model to investigate the storage capacity of coalbeds by considering different factors. Their hydraulic−mechanical−thermal-coupled model considered dual porosity characteristics of coal seams and non-isothermal conditions. The assumptions used during model development are the following: (1) Free gas occurs in fracture and matrix. (2) Coal seam matrix and fracture systems have steady structures having equal initial porosity and gas pressure. (3) The gas in the coal seams is assumed to be an ideal gas. (4) The fracture and matrix system are governed by different transport equations, but exchange occurs in between. (5) The sorption process occurs instantaneously with the single gas component considered. (6) Coal deformation is a reversible process. It was revealed that after CO_2 injection, the permeability was reduced due to swelling and shrinkage of coal seams caused by pressure increase and matrix expansion caused by the rise in temperature. Furthermore, it was discovered that the higher the initial temperature of the coal seam, the less CO_2 adsorbed, and in the presence or development of fractures in the coal seam, the higher the CO_2 seepage rate and, therefore, CO_2 sequestration.

Moreover, ref 101 modeled and optimized CO_2 sequestration and CH_4 recovery in deep unmineable coal seams by injecting CO_2/N_2 mixtures. A developed improved thermo-hydro-mechanical (THM) model involved complex interaction between the ternary gas systems (CO_2, CH_4, N_2) such as heat transfer, mass transport between two-phase flow, coal deformation, and sorption process in coal seams. After the validation, the model was used to simulate the most important parameter for gas mixture-enhanced coalbed methane (GM-ECBM) technology application. The developed model assumed that (1) Coal seam was considered to have elastic single permeability and dual porosity between fractures and matrix. (2) The ternary gas obeys the ideal gas law. (3) Ternary gases are adsorbed on the inner surface of the matrix while free gases and water migrate through the fractures. (4) Ternary gases and water mixtures occupy the coal seam fractures. (5) The mass transport of ternary gases in coal seams occurs in three steps consecutively, i.e., first, CH_4 desorbs from the coal surface, obeying the modified Langmuir equation, and then flows through fractures sustaining Fick's law. Finally, CH_4 flows to the production well to satisfy Darcy's law. The results revealed that after injecting the CO_2/N_2 mixture into coal seams, cumulative CH_4 production increased compared to conventional production, with cumulative CO_2 sequestrated reaching to 13.83×10^6 m^3 for 6000 days, with an optimal injection ratio of 15:85 for CO_2:N_2. Also, ternary gas injection increases permeability after CH_4 desorption in the initial days; then, permeability declined rapidly due to coal swelling after CO_2 adsorption. However, the main challenge was the N_2 early breakthrough which can lead to increased costs during gas processing. It was suggested that to increase the amount of sequestrated CO_2, the ratio of CO_2 in the injector stream should be greater than N_2; nevertheless, it will result in lower CH_4 production.

Furthermore, ref 119 modeled and simulated CO_2 sequestration potentiality in deep unmineable coal seams at the Allison unit for CO_2-ECBM pilot tests. In their study, COMET3 was used for reservoir modeling and simulation in which the future performance of the coal field was predicted through history matching. The results revealed that after injecting 1.8×10^8 tonnes of CO_2 into coal seams, 1.3×10^8 tonnes were sequestrated. The CH_4 production increase could help offset the associated costs for carbon capture, separation, and transportation to make the CO_2-ECBM project feasible. In addition, there was clear evidence of permeability reduction during CO_2 injection, which will hinder CH_4 production and make the project uneconomical. Future researchers need to consider good ways of preventing permeability reduction effects. Also, ref 109 established a fully coupled hydromechanical model to investigate CO_2 sequestration in deep unmineable coal seams by considering various mechanisms (cross couplings). The developed model was validated by using the multiphysics software COMSOL. The results revealed that the newly developed model could model long-term CO_2 sequestration in coal seams at the early injection stage. Most of the injected gas was stored in the adsorbed state ($\sim 14.1 \times 10^5$ m^2); after that, CO_2 was stored in a free state ($\sim 8 \times 10^5$ m^2). In addition, it was found that long-term CO_2 sequestration is better in coal seams with higher CO_2 diffusion attenuation coefficients, especially when the model considers gas dynamic diffusion.

Moreover, ref 120 used the coal inventory calculation (KVD) model to estimate the CO_2 sequestration capacity of deep unmineable coal seams of the Munster Cretaceous Basin of North Rhine-Westphalia, Germany. By assuming that 40% of the total area is accessible, the CH_4 recovery was estimated to be 80% of the maximum CO_2 stored of 160 million tonnes for coal seams below the 3000 m depth. Due to the low permeability of the study area at larger depth, the CO_2-ECBM technology applications are less successful. It was found that deep unmineable coal seams with <1 mD permeability and depth of >1500 m are not recommended for CO_2-ECBM technology application because low permeability reduces injection rate. Hence, to meet the minimum injection rate, it will require drilling multiple wells, which is expensive and will make a project uneconomical. Thus, more research is needed to innovate injection technology of CO_2 in coal seams with <1 mD permeability and depth of >1500 m. In addition, ref 121 investigated the CO_2 sequestration potentiality and CH_4 production using a 3D stochastic reservoir model and

https://doi.org/10.1021/acs.energyfuels.3c03004
Energy Fuels XXXX, XXX, XXX−XXX

simulations of the Big George coal, Powder River Basin, Wyoming, USA. The simulation results revealed that 99% of the total injected CO_2 was sequestrated, with CH_4 production increased 5 times compared to that before CO_2 injection.

In addition, ref 103 did a numerical simulation on CO_2 sequestration and CH_4 recovery using the multiphysics software COMSOL in deep unmineable coal seams utilizing CO_2-ECBM technology. The hydraulic−mechanical−thermal-coupled model built considered gas seepage and adsorption, coal deformation, and thermal exchange. The assumptions used in model development were the following: (1) The coal seam is homogeneous isotropic. (2) The coal matrix deformation is elastic (small deformation). (3) Coal bed methane is evenly distributed. (4) The gas in coal is ideal. (5) Pore pressure is negative, whereas tensile stress is positive. The injection pressure and initial reservoir temperature effects on CO_2 sequestration were evaluated. It was found that the higher injection pressure results in higher CO_2 sequestration, whereas the higher initial reservoir temperature results in lower CO_2 sequestration, as shown in Figures 8 and 9,[103] respectively. On the other hand, initial low reservoir temperature condition results in higher CH_4 production, while high injection pressure results in high CH_4 production.

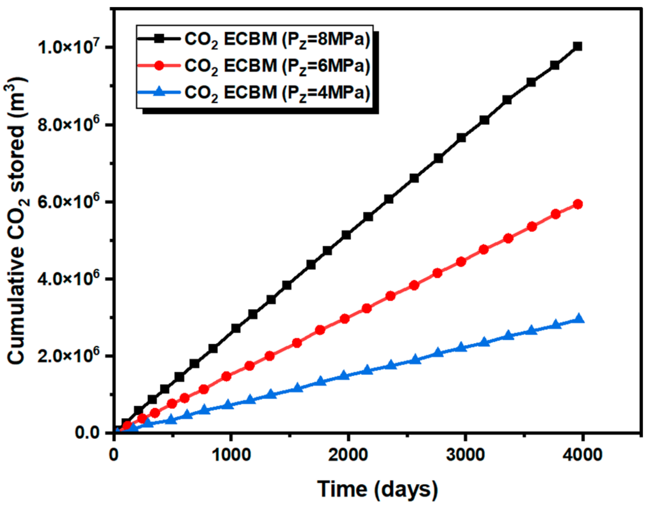

Figure 8. Injection pressure effects on CO_2 sequestration. This figure was reproduced with permission from ref 103. Copyright 2018 Elsevier.

Furthermore, ref 122 investigated CH_4 recovery and CO_2 sequestration in low-permeability coal reservoirs in the southeastern Qinshui Basin, Shanxi Province, China, using a numerical simulator. The developed model assumed that (1) Coal is assumed to have dual porosity having a matrix and fracture system. (2) Migration of gas in the matrix ensures Fick's law. (3) Water and gas flows in the fracture systems are laminar and follow Darcy's law. (4) The coal seams are isothermal, i.e., the temperature effect was ignored. A COMET3 commercial reservoir simulator was used in their study for numerical computations. The results revealed that 99.9% of injected CO_2 was sequestrated. Also, ref 123 did 3D numerical simulations on assessing the performance of horizontal and vertical injectors in sequestrating CO_2 in deep unmineable coal seams located in Indonesia Basins using CMG-GEM. The results revealed that a horizontal well sequestrated CO_2 three times compared to a vertical well. Several sorption models have been applied during modeling and simulation in deep coal mineable seams during

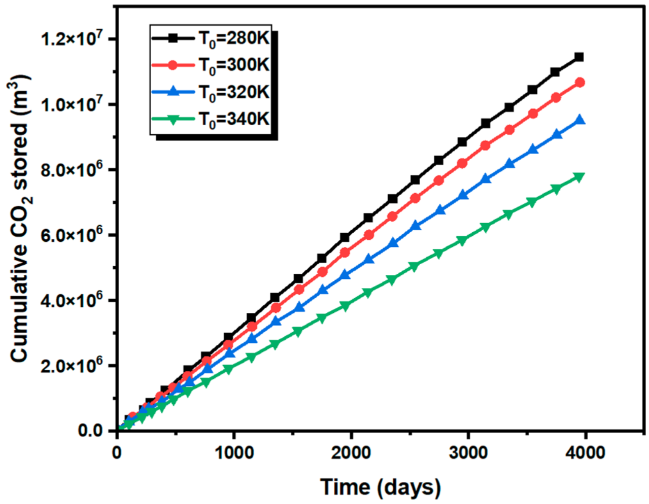

Figure 9. Initial reservoir temperature influence on CO_2 sequestration. This figure was reproduced with permission from ref 103. Copyright 2018 Elsevier.

CO_2-ECBM technology application for CO_2 sequestration and CH_4 production purposes, as shown in Table 6. However, it has been found that the most accurate model to estimate the amount of adsorbed gas in coal seams is the D−A model compared to others because it may derive isotherms for any temperature employing a single isotherm, making it easier to describe injection/depletion-induced temperature change.[124] A summary of modeling and simulation studies on CO_2-ECBM technology application for CO_2 sequestration is shown in Table 7.

In Table 6 V is adsorbed gas volume, m^3/kg; V_L is the volume constant of the Langmuir equation, namely, the adsorbed gas volume under saturated pressure, m^3/kg; P is the pressure of the gas, MPa; b is the pressure gas constant, MPa^{-1}; c_1 is the temperature coefficient, K^{-1}; c_2 is the pressure coefficient, Pa^{-1}; $p_m = p_{mg1} + p_{mg2}$, which is the gas pressure in the coal matrix, Pa; T_{ref} is reference temperature, K; R is the universal molar gas constant, J $mol^{-1}K^{-1}$; T is the temperature of the adsorbate, K; E_g is the characteristic energy of the adsorbent; β is the affinity coefficient of the adsorbate; n is the structural heterogeneity parameter; n is the available space for adsorption, n_0 is the maximum number of available sites for adsorption; P_0 is the saturation pressure; ρ_{free} is the density of gas at the free phase; $\rho_{absorbed}$ is the density of gas at the adsorbed phase; π_i^* is the decreased spreading pressure of component i ;$n(P)$ is adsorption of the pure component at pressure P; A is the adsorbent surface area.

6. FIELD APPLICATIONS

Notwithstanding various theories, experiments, a few models and simulations, and a few pilot tests exploring CO_2-ECBM technology application on CO_2 sequestration and enhancing CH_4 recovery, there has been no full field implementations of this technology. This is accredited to numerous challenges, such as permeability reduction due to swelling and shrinkages after CO_2 adsorption into the coal surface and reduction of fracture pore space, resulting in a lower production rate and difficulty injecting CO_2. Another big challenge is an uneconomical issue, regardless of helping to preserve the environment through CO_2 sequestration. Some major pilot tests where CO_2-ECBM technology has been executed are elucidated in this section.

https://doi.org/10.1021/acs.energyfuels.3c03004
Energy Fuels XXXX, XXX, XXX−XXX

Table 6. Comparison of Gas Sorption Models for Deep Unmineable Coal Seams

model name	characteristics	equations	limitations	references
		Sorption Models for Single Gas Components		
Langmuir model	monolayer adsorption process; adsorption only occurs only when empty adsorption sites are available	$\frac{V_L P}{P_L + P}$	does not consider the heterogeneous surface; does not work for a complex system with multiple adsorbents; did not consider temperature effects which are an important factor in the adsorption process.	125
BET model	multilayer adsorption process	$n = \frac{n_0 c\left(\frac{P}{P_0}\right)}{\left(1 - \left(\frac{P}{P_0}\right)\right)\left(1 + (C-1)\left(\frac{P}{P_0}\right)\right)}$	model assumes that there is no interaction between the adsorbent surface and adsorbate molecules; did not consider temperature effects, which are an important factor in the adsorption process; limited to homogeneous adsorbents	126
Dubinin−Astakhov (D−A) model	micropore volume filling	$V = V_0 \exp\left\{-\left(\frac{RT}{\beta E_g}\ln\frac{P}{P_0}\right)^n\right\}$	model works only for adsorbate with low adsorption energies, not suitable for the chemisorption process; limited temperature dependency	127, 128
		Sorption Models for Multiple Gas Components		
ideal adsorbed solution (IAS) theory	describes the adsorption behavior of components in a mixture onto a solid adsorbent surface	$\pi_i^* = \frac{\pi A}{RT} = \int_0^P \frac{n(P)}{P}\mathrm{d}P$	it does not consider heterogeneous surfaces; not suitable for nonideal adsorption systems; no surface coverage dependency	129
high-pressure Langmuir model	incorporates the influence of high pressures on adsorption behavior	$V = \frac{V_L}{P_L + P}\left(1 - \frac{\rho_{free}}{\rho_{adsorbed}}\right)$	incomplete description of multilayer adsorption; it does not consider heterogeneous surfaces; limited temperature dependency	130, 131
extended Langmuir model I	gases mixtures are evenly distributed on the adsorbent	$V_i = \frac{V_L b_i P_i}{1 + \sum_{i=1}^{2} b_i P_i}$	not suitable for strongly adsorbing systems; limited temperature dependency; no interaction between adsorbed layers	132
extended Langmuir model II	nonisothermal adsorption process	$V_{sgi} = \frac{V_L b_i P_{mgi}}{1 + \sum_{i=1}^{2} b_i P_{mgi}} \exp\left\{-\frac{c_1}{1 + c_2 p_m}(T - T_{ref})\right\}$	it does not consider heterogeneous surfaces; not suitable in systems with nonuniform or varying adsorbate−adsorbent interactions; not suitable for strongly adsorbing systems	113

https://doi.org/10.1021/acs.energyfuels.3c03004
Energy Fuels XXXX, XXX, XXX−XXX

Table 7. Summary of Modeling and Simulations Studies on CO_2-ECBM Technology Applications

author(s)	objectives	software or model used	key findings
118	predicting the storage capacity of the Ishikari coal field using laboratory data	Ishikari model	72% of injected CO_2 gas can be stored during the huff and puff test. 96% of injected CO_2 can be stored for a multiwell test. In general, it was predicted that 1.2×10^6 tonnes of CO_2 can be stored in the Ishikari coal field. The CH_4 production rate increased from 500 to 1300 m^3/day during CO_2 injection.
101	to investigate the storage capacity of coalbeds by considering the hydraulic–mechanical–thermal-coupled model and dual porosity characteristics of coal seams and nonisothermal conditions	hydraulic–mechanical–thermal-coupled model	After CO_2 injection, the permeability was reduced due to swelling and shrinkage of coal seams caused by pressure increase and matrix expansion caused by the rise in temperature. The higher the initial temperature of the coal seam, the less CO_2 adsorbed.
101	optimizing CO_2 sequestration and CH_4 recovery in deep unmineable coal seams by injecting CO_2/N_2 mixtures	improved thermo-hydro-mechanical (THM) model	Injecting the CO_2/N_2 mixture into coal seams, cumulative CH_4 production increased compared to conventional production, with cumulative CO_2 sequestrated reaching to 13.83×10^6 m^3 for 6000 days, with an optimal injection ratio of 15:85 for CO_2:N_2. To increase CO_2 sequestration, the injector stream CO_2 ratio should be bigger than N_2; however, it will limit CH_4 generation.
119	simulated CO_2 sequestration potentiality in deep unmineable coal seams at the Allison unit	COMET3	-1.8×10^8 tonnes of CO_2 were injected into coal seams with 1.3×10^8 tonnes sequestrated. There was clear evidence of permeability reduction during CO_2 injection, which will hinder CH_4 production and make the project uneconomical.
109	establish a fully coupled hydromechanical model to investigate CO_2 sequestration in deep unmineable coal seams by considering various storage mechanisms	COMSOL	Most CO_2 stored in the adsorbed state ($\sim 14.1 \times 10^5$ m^2). Other injected CO_2 was stored as the free state ($\sim 8 \times 10^5$ m^2).
120	estimating the CO_2 sequestration capacity of deep unmineable coal seams of the Munster Cretaceous Basin of North Rhine-Westphalia, Germany	coal inventory calculation (KVD) model	CH_4 recovery was estimated to be 80% of the maximum CO_2 stored of 160 million tonnes for coal seams. Deep unmineable coal seams with <1 mD permeability and depth of >1500 m are not recommended for CO_2-ECBM technology application because low permeability reduces injection rate.
121	to investigate the CO_2 sequestration potentiality and CH_4 production in coal seams	3D stochastic reservoir model	99% of the total injected CO_2 was sequestrated, with CH_4 production increased 5 times compared to that before CO_2 injection.
103	to investigate the CO_2 sequestration potentiality and CH_4 production in coal seams	COMSOL	Cumulative CO_2 stored increased as the injection pressure increased, i.e., At 8 MPa the CO_2 stored was 1×10^7 m^3 while at 4 MPa cumulative CO_2 sequestrated was 2×10^6 m^3. Low reservoir temperature results in high CO_2 storage compared to high temperature, i.e., 1×10^7 m^3 at 280 K and 6.1×10^6 m^3 at 340 K.
122	to examine the CH_4 recovery and CO_2 sequestration in low-permeability coal reservoirs in the southeastern Qinshui Basin, Shanxi Province, China	COMET3	99.9% of injected CO_2 was sequestrated.
123	to assess the performance of horizontal and vertical injectors on sequestrating CO_2 in deep unmineable coal seams located in Indonesia Basins	CMG-GEM	Horizontal well sequestrated CO_2 three times compared to a vertical well.

https://doi.org/10.1021/acs.energyfuels.3c03004
Energy Fuels XXXX, XXX, XXX−XXX

Table 8. Summary of Global Pilot Tests of CO_2-ECBM Technology Applications

field location	coal rank	CO_2 phase injected	challenges	CO_2 sequestrated	monitoring techniques	references
Deep Mannville coal, Mikwan area, near Red Deer, Alberta, Canada, February 2022 to March 4, 2022	bituminous	CO_2	permeability reduction	1512 tonnes of CO_2 were injected for 8 days	sensors	150
Marshall County Coalfield, USA, September 2009 to December 2013	bituminous	CO_2	pump failure, permeability reduction, early CO_2 breakthrough	4500 tonnes of CO_2 were injected with 78.2% sequestrated	soil gas monitoring, seismic and tiltmeter observations, produced water and gas, ground and streamwater monitoring	133
San Juan County coal field, USA, April 1995 to August 2001	bituminous	liquid CO_2	permeability reduction by 18%	1.5×10^8 tonnes of CO_2 were injected with 1.1×10^8 tonnes of CO_2 sequestrated	gas composition	119
Ishikari coal field, Hokkaido, Japan, late 2004 to September 2007	high-volatile bituminous	liquid CO_2	well damage due to fine coal particle migration, permeability reduction from 1 to 0.08 mD during injection and 0.01 mD during shut-in	800 tonnes of CO_2 were injected with 98% sequestrated	pressure and gas composition	134−136
Fenn Big Valley, Alberta, Canada, 1992−1993	high-volatile C/B bituminous	liquid CO_2	permeability reduction	201 tonnes of CO_2 were injected with 70% stored	pressure and gas composition	137,138
Liulin County, Shanxi Province, China, September 2011 to March 2012	medium-volatile bituminous	liquid CO_2	permeability decline during injection, early CO_2 breakthrough	460 tonnes of CO_2 were injected with 88% sequestrated	U-tube system, vertical well monitoring placed 20 m from the injector	139
Southern Shizhuang, Qinshui Basin, China, April−June 2004	anthracite	liquid CO_2	permeability decline during injection, early CO_2 breakthrough, burst of tubings, failure of pumps due to plugging	192 metric tonnes of CO_2 were injected in 13 days, with 30% stored in the first month; then, stored CO2 increased to 45%.	pressure and gas composition, water chemistry	28
Northern Shizhuang, Qinshui Basin, China, April 2010 to May 2010	anthracite	liquid CO_2	permeability decline during injection, early CO_2 breakthrough	233.6 metric tonnes of CO_2 were injected, with 51% stored.	pressure and gas composition	140
Northern Shizhuang, Qinshui Basin, China, 2013−2015	anthracite	liquid CO_2	permeability reduction; early CO_2 breakthrough	4491 tonnes of CO_2 were injected with approximately 70% stored	water sampling, transient electromagnetic	141
San Juan Basin, USA, July 2008 to August 2009	bituminous	CO_2	permeability reduction	16 699 tonnes of CO_2 were injected with approximately 80% stored	water chemistry, gas composition	142
Wabash County, USA, June 2008 to January 2009	high-volatile bituminous	liquid CO_2	permeability reduction	0.378 tonnes of CO_2 sequestrated from 92.3 tonnes of injected CO_2	groundwater CO_2 levels, atmospheric shallow	143, 144
Central Appalachian Basin, USA, January 2009 to February 2009	bituminous	CO_2	permeability reduction	907.185 tonnes of CO_2 were injected with 65% sequestrated	pressure and gas composition	133, 145
Tuscaloosa County, USA, June 2010 to August 2010	bituminous	liquid CO_2	permeability reduction	252 tonnes of CO_2 were injected with greater than 50% stored	water and gas composition, pressure logging	146, 147
Buchanan County, United States, July 2015 to September 2017	bituminous	CO_2	permeability reduction	12 032 tonnes of CO_2 were injected with 87% stored	microseismic and surface deformation measurement, gas/water composition, tracers/isotopes, well logging	146
Kaniow village, Poland, August 2004 to May 2005	high-volatile bituminous	liquid CO_2	permeability reduction	689 tonnes of CO_2 were injected with 628 tonnes stored	water chemistry, gas composition, isotopes	148, 149
RECOPOL, Silesian Basin of Poland, July 2005 to June 2005	bituminous coal seams	CO_2	permeability reduction	760 tonnes of CO_2 were injected	tracers/isotopes, geochemical	151
MOVECBM, Velenje coal mine (Slovenia)	lignite	CO_2	permeability reduction	0.0057 tonnes were injected for 26 h	tracers/isotopes, geochemical	151
CARBOLAB, Montsacro Pit in Asturias (North of Spain), 2009−2013	bituminous coal seams	CO_2	permeability reduction	0.12 tonnes of CO_2 were injected for 2 months	stress-state analysis, geochemical, passive seismic, geophysical	151, 152

https://doi.org/10.1021/acs.energyfuels.3c03004
Energy Fuels XXXX, XXX, XXX−XXX

A pilot test was carried out in the USA to demonstrate the effectiveness and economics of using horizontal wells in CO_2 sequestration and CH_4 production in deep unmineable coal seams by using ECBM technology in Marshall County, West Virginia. 4500 tonnes of CO_2 were injected at a rate of 7.63−8.39 tonnes per day at an injection pressure of 6.8−7.7 MPa. It was revealed that approximately 78.2% of the CO_2 injected was sequestrated. The major challenges faced were pump failure during injection and permeability decline caused by coal swelling after CO_2 adsorbed into the coal surface. Also, it was found that down-dip drilling is not suitable for CBM wells.[133] Furthermore, a field trial in San Juan county, New Mexico, revealed that injecting CO_2 in the liquid phase during CO_2-ECBM in the Allison unit CBM site is possible. In this pilot test, 1.5×10^8 tonnes of CO_2 were injected with 1.1×10^8 tonnes of CO_2 sequestrated. In addition, it was found that 18% of the permeability of formation was reduced after CO_2 injection, which creates difficulty in the injection process and CH_4 production.[119]

Moreover, another field test was conducted at Ishikari coal field, Hokkaido, in Japan, where approximately 800 tonnes of liquid CO_2 were injected at a rate of 1.7−3.8 tonnes per day with a bottom pressure range of 15.5−19 MPa. It was found that 98% of injected CO_2 was sequestrated, and CH_4 production increased.[134−136] Furthermore, in Fenn Big Valley, Alberta, Canada, 201 tonnes of liquid CO_2 were injected at a rate of 48−96 tonnes per day at a maximum injection pressure of 2.7−6.1 MPa. It was found that more than 70% of injected CO_2 was sequestrated, and CH_4 production increased compared to conventional production techniques.[137,138] Also, in Liulin County, Shanxi Province, China, a pilot test was conducted to investigate the CO_2 sequestration effectiveness in deep unmineable coal seams using a multilateral horizontal injection well. 460 tonnes of liquid CO_2 were injected for 70 days at an injection rate of 48 tonnes per day at a bottom hole pressure of 5.5 MPa. It was reported that 12% of injected CO_2 was sequestrated, with the rest recovered with CH_4.[139]

Additionally, 192 tonnes of liquid CO_2 were injected at South Qinshui, Shanxi, China, for 13 days at an injection rate of 36−54 tonnes per day at a maximum injection pressure of 6.7 MPa. It was revealed that in the first 13 days, 30% of injected CO_2 was sequestrated, and then later CO_2 stored increased to 45%.[28] In addition, 233.6 tonnes of liquid CO_2 were injected in Northern Shizhuang, Qinshui Basin, China, at a maximum injection pressure of 7 MPa. It was revealed that 51% of injected CO_2 was sequestrated.[140] Moreover, in Northern Shizhuang, Qinshui Basin, China, a pilot test was conducted in which 4491 tonnes of liquid CO_2 were injected for 460 days at an injection rate of 30−31.2 tonnes per day with a maximum injection pressure of 6.2−6.7 MPa. It was found that 70% of injected gas was sequestrated.[141] In addition, a pilot test was conducted in Pump Canyon, San Juan Basin, New Mexico, to investigate CO_2 sequestration. 16 699 tonnes of liquid CO_2 were injected at 1.06×10^5 to 1.4×10^4 tonnes daily with a bottomhole pressure (BHP) of 7.7 MPa. It was revealed that 80% of injected CO_2 was sequestrated.[142] Further, in Wabash County, United States, 92.3 tonnes of liquid CO_2 were injected at a rate of 0.93 tonnes per day with a maximum injection pressure of 5.34 MPa. The results revealed that 0.387 tonnes of CO_2 were sequestrated, which was very low compared with the predicted one from the Langmuir isotherm.[143,144]

Besides that, a pilot test was conducted in the Central Appalachian Basin, United States, in which 907.185 tonnes of CO_2 were injected at a rate of 36−45 tonnes per day in the initial days and then later decreased to 20 tonnes per day at a maximum injection pressure of 6.9 MPa. It was revealed that 65% of injected CO_2 was stored.[133,145] Also, 252 tonnes of liquid CO_2 were injected in Tuscaloosa County, Alabama, United States, at an injection rate of 113−136 tonnes per day with a bottom hole pressure of 7.1 MPa. It was found that >50% of injected CO_2 was sequestrated.[146,147] Moreover, in Buchanan County, Virginia, United States, 12 032 tonnes of CO_2 were injected at an injection rate of 4.5−22.5 tonnes per day with a maximum injection rate of 1.7−2.9 MPa. It was revealed that 87% of injected CO_2 was sequestrated.[146] In addition, 689 tonnes of liquid CO_2 were injected in Kaniow village, Poland, which were injected at a rate of 1−1.3 tonnes per day before hydraulic fracturing and 12−15 tonnes per day after hydraulic fracturing with a maximum injection pressure of 14.0 MPa. It was found that 628 tonnes of CO_2 were sequestrated.[148,149] Table 8 summarizes the pilot tests for CO_2-ECBM technology application for CO_2 storage in deep unmineable coal seams.

7. WETTABILITY ALTERATION DURING CO_2-ECBM TECHNOLOGY APPLICATION

The CO_2 sequestration and CH_4 recovery effectiveness on coal seams depend on wettability changes of the CO_2−H_2O−coal system.[153−155] CO_2 diffusion is very fast for hydrophobic coal because it fills the small pores in the coal surface compared to hydrophilic coals. The CO_2 diffusion rate is 1.7×10^{-7} m^2 /s for hydrophobic coal, while for hydrophilic coal the CO_2 diffusion rate is 2×10^{-9} m^2/s at 100 bar and 300 K.[156−158] Fluid interactions during CO_2-ECBM technology applications are very important in enhancing CH_4 production and CO_2 sequestration. Fluid interactions alter the wettability of the unmineable coal seams. Wettability alterations can be due to either CO_2−H_2O or CO_2−CH_4 interactions.[159] Wettability alteration influences both gas sorption and transport mechanisms. The sorption and transport mechanisms are controlled by reservoir temperature, injection pressure, and the existing state of water (free or adsorbed water). Reference 160 experimented on the dynamic interactions of CO_2−H_2O in anthracite and sub-bituminous coals using nuclear magnetic resonance (NMR). It was revealed that the existence of free water in coals decreases the wettability alterations (CO_2 sorption capacity), thus resulting in little CH_4 production and CO_2 sequestration. The dewatering process must be applied first to improve storage capacity and production because it helps to improve gas transport during injection and production and increases CO_2 wettability. Also, CO_2 wettability changes of coals increase with the surge in CO_2 injection pressure to not more than 5 MPa, while CO_2 wettability increases with a diminution in temperature which will help to enhance CO_2 sequestration and CH_4 production. In addition, ref 87 investigated the wettability change effects on the CO_2−H_2O−coal system to influence CO_2 sequestration and CH_4 recovery by measuring the water contact angle using the pendent drop tilted place method for three coal ranks. The influence of temperature, pressure, and salinity was also observed. The results revealed that high coal rank has high sorption capacity (strongly CO_2-wet), followed by low coal rank (medium CO_2-wet) and medium coal rank (weak CO_2-wet). Also, the CO_2 wettability increased with the increase of pressure and salinity while decreasing with an increase in temperature. This proves that high-rank coals are the best candidates for CO_2 sequestration and CH_4 recovery at high pressure and low temperature due to increased CO_2 wettability. Similar results

https://doi.org/10.1021/acs.energyfuels.3c03004
Energy Fuels XXXX, XXX, XXX−XXX

were reported by ref 161. However, they found that injecting liquid and Sc-CO_2 influenced CO_2 wettability compared to CO_2 gas. Nevertheless, the coal rank is the greatest parameter controlling the coal wettability change.[162−164]

7.1. Coal Wettability Alteration Prediction for CO_2 Sequestration. Machine learning (ML) has been employed in various sectors, such as oil and gas and the environmental sector. Different ML like artificial neural networks (ANN), group methods of data handling (GMDH), adaptive neuro-fuzzy inference systems (ANFIS), function networks (FN), support vector machines (SVM), Gaussian process regression (GPR), random forest (RF), regression tree ensembles, deep neural networks, convolution neural networks (CNN), long short-term memory (LSTM) network, etc., can be used to predict certain parameters from easily available data without incurring additional costs.[165−171] Due to the fact that the capacity of coal to sequestrate CO_2 depends on the wettability of the formation, which is measured by contact angle (CA), ref 172 predicted the CA of coal formation toward CO_2 wetness, implying that CO_2 sorption capacity increases as the CA angle increases. The ML techniques used were ANN and ANFIS. The inputs used for the model's developments were pressure (P), ash content (AC%), moisture content (MC%), temperature (T), volatile content (VC%), maximum vitrinite reflectance (R_{max}), and fixed carbon mass concentration (FC%), while the output of the model was CA. 250 data points were obtained from various published sources, with 70−90% of the data used for training and the rest used for testing. The correlation coefficient (R) and average absolute percent error (AAPE) were 0.98 and 4.2% for ANN and 0.98 and 3% for ANFIS during training, respectively. For testing, R and AAPE were 0.96 and 7% for ANN and 0.97 and 5.6% for ANFIS, respectively. These results confirm that the ANFIS model outperformed the ANN model in CA prediction. This shows the applicability of machine learning in predicting the carbon dioxide sequestration capacity, which depends on wetness and CA measurements. In general, as CA becomes high, CO_2 wetness (CO_2 sorption capacity) into the coal surface increases; consequently, CO_2 sequestration increases in coal formation. Furthermore, sensitivity analysis (SA) revealed that ML could predict CA with R of 0.95−0.98 and AAPE of ±6% with the minimum number of input parameters such as pressure, temperature, and coal properties (AC% and R_{max}).

Also, ref 173 predicted the CA of coal formation toward CO_2 wetness, implying that CO_2 sorption capacity increases as the CA angle increases. The ML techniques used were FN, SVM, and RF. The ML techniques used were ANN and ANFIS. The inputs used for the model's developments were pressure (P), ash content (AC%), moisture content (MC%), temperature (T), volatile content (VC%), maximum vitrinite reflectance (R_{max}), and fixed carbon mass concentration (FC%), while the output of the model was CA. 250 data points were obtained from various published sources, with 70−90% of the data used for training and the rest used for testing. The R and AAPE were 0.97 and 4.5% for FN, 0.95 and 6.5% for SVM, and 0.99 and 2.2% for RF during training, respectively. For testing, R and AAPE were 0.97 and 7% for FN, 0.96 and 6.4% for SVM, and 0.97 and 7% for RF, respectively. These results show the efficient applicability of machine learning in predicting the carbon dioxide sequestration capacity, which depends on wetness and CA measurements. From sensitivity analysis between inputs and output, P, FC, and R_{max} show a positive, strong relationship with CA, while the remaining inputs have a negative relationship with CA. The developed ML models can generally replace experimental parts on CA of coal−H_2O−CO_2 measurements, which is important for CO_2 sequestration application.

Furthermore, ref 174 predicted the CA of coal formation toward CO_2 wetness, implying that CO_2 sorption capacity increases as the CA angle increases. The ML techniques used were LR, XGBoost model, and RF. The ML techniques used were ANN and ANFIS. The inputs used for the model's developments were pressure (P), ash content (AC%), moisture content (MC%), temperature (T), volatile content (VC%), maximum vitrinite reflectance (R_{max}), and fixed carbon mass concentration (FC%), while the output of the model was CA. 250 data points were obtained from various published sources, with 70−90% of the data used for training and the rest used for testing. The R and AAPE were 0.86 and 13% for LR, 0.99 and 3.4% for XGBoost, and 0.99 and 2.2% for RF during training, respectively. For testing, R and AAPE were 0.87 and 13% for LR, 0.96 and 6.2% for XGBoost, and 0.97 and 7% for RF, respectively. These results prove that XGBOOST and RF models could predict the CA of the coal−H_2O−CO_2 system with minimum error compared to LR. In general, the developed ML models can replace experimental parts of the CA of coal−H_2O−CO_2 measurements, which is important for CO_2 sequestration application.

8. NANOTECHNOLOGY APPLICATION DURING CO_2 SEQUESTRATION IN SHALLOW CBM RESERVOIRS

Recently, nanotechnology application in CCS has been increased due to its unique properties, such as high surface energy, low sorbent cost, regeneration, simplicity of design, and high selectivity. This section discusses a few literature studies which investigated applications of various nanomaterials that can enhance carbon dioxide sequestration in CBM.

Reference 175 conducted an experiment to investigate the effects of nanoparticle application in CO_2 sequestration in shallow CBM reservoirs (<300m). Different rice husk silicas (RSi) were used to observe their effects on enhancing sorption capacity, which was synthesized from a local Colombian mill. RSi was modified by adding nitrogen compounds, i.e., urea (U), ethylenediamine (EM), triethylamine (TE), and diethylamine (DE), to form four different nanoparticles such as RSi-U, RSi-EM, RSi-TE, and RSi-DE, as shown in Figure 10. Different mass fractions of 1, 3, and 5 wt % of modified nanoparticles were used during the experiments. Sorption experiments were conducted

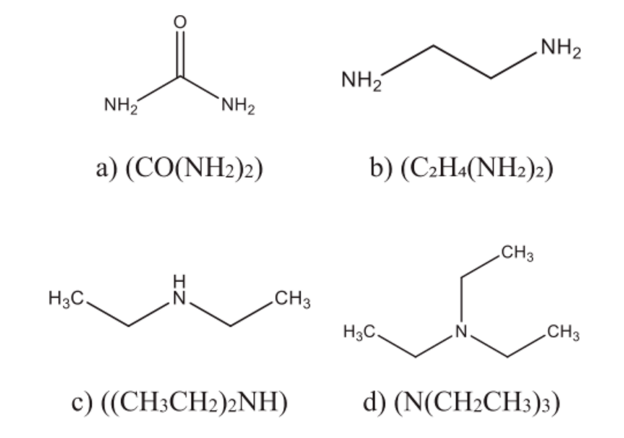

Figure 10. Chemical structures of used modifiers: (a) urea, (b) ethylenediamine, (c) diethylamine, and (d) triethylamine. This figure was reproduced with permission from ref 175. Copyright 2023 American Chemical Society.

https://doi.org/10.1021/acs.energyfuels.3c03004
Energy Fuels XXXX, XXX, XXX−XXX

using a thermogravimetric equipment (HP-TGA 750) analyzer in different temperature and pressure conditions, i.e., 30 °C and 0.084−3 MPa, to select the best nanoparticles for enhancing CO_2 sequestration in CBM. The results revealed that CO_2 sorption capacity increases as RSI increases with nitrogen group order increase, i.e., RSi-EM > RSi-U > RSi-TE > RSi-DE. Also, as the mass fraction of modifiers increases to nanoparticles, the CO_2 sorption capacity increases; however, 5 wt % leads to nanoparticle agglomeration, which decreases CO_2 adsorption capacity due to porous structure blockage. In addition, for the context of CBM impregnation, it was observed that the nanofluids, including 20 wt % of RSi-EM3, exhibited the greatest efficiency in enhancing CO_2 sorption. Specifically, the sorption capacity increased from 0.05 to 0.75 mmol g^{-1}, representing a remarkable augmentation of over 1000% in the overall sorption capability.

Also, ref 176 did an experiment to examine the potential impacts of nanoparticle utilization on CCS in shallow coalbed methane (CBM) sandstone reservoirs collected from the Ottawa field to reflect field reality. Various types of nanoparticles were utilized to investigate their impact on improving sorption capacity originating from carbon nanostructures. These carbon nanostructures include CN.LYS and CN.MEL, which were synthesized using the sol−gel and solvothermal methods, respectively. The investigations involved the utilization of carbon nanostructures with varying mass fractions, specifically 0.01, 0.1, 1, 5, and 20 wt %, which were impregnated within Ottawa sandstone reservoir designed at a shallow depth of <300 m by soaking and immersion. In their experiment, the carbon capture facilities were removed; instead, carbon was injected directly into the reservoir. Sorption examinations were conducted with a thermogravimetric analyzer (HP-TGA 750) at various temperatures and pressure circumstances, namely, at 0, 25, and 50 °C and within the range of 0.003−3 MPa, respectively, for CO_2 and N_2. The findings of the study indicate that N_2 rich carbon nanostructures of CN.LYS increased adsorption capacity by 67 700% compared to other nanostructures when 20 wt % mass fraction was used under actual reservoir conditions of 50 °C and 3 MPa because it has a larger surface area and favorable chemical composition, which made them have higher adsorption capacity compared to others.

Moreover, ref 177 did an experiment to investigate the potential influence of nanoparticle utilization on CCS in shallow coalbed methane (CBM) sandstone reservoirs collected from the Ottawa field to reflect field reality. Various types of nanoparticles were utilized to investigate their impact on improving sorption capacity originating from carbon latex spheres. These nanoparticles include carbon spheres from resorcinol/formaldehyde (CN.POL) and carbon spheres from cane molasses (CN.RON). The investigations involved the utilization of carbon nanostructures with varying mass fractions, specifically 10 and 20 wt %, which were impregnated within the Ottawa sandstone reservoir with CN. RON2 was designed at a shallow depth of <300 m by soaking and immersion. In their experiment, the carbon capture facilities were removed; instead, carbon was injected directly into the reservoir. Sorption examinations were conducted with a thermogravimetric analyzer (HP-TGA 750) at 25 and 50 °C temperatures and within the pressure range of 0.03−3 MPa, respectively, for CO_2 and N_2 sorption. The findings of the study indicate that CN.RON2 increased the adsorption capacity by 730% when 20 wt % mass fraction of CN.RON2 was utilized under actual reservoir conditions of 50 °C and 3 MPa due to its favorable physical structure and chemical composition that enhanced adsorption capacity compared to others.

However, most of the researchers developed nanomaterials for the carbon capture and separation process toward carbon sequestration.[178−185] It is recommended to develop nanomaterials specifically to enhance CO_2 sequestration in CBM for shallow and deep reservoirs.

9. ESTIMATION OF CO_2 STORAGE CAPACITY IN DEEP UNMINEABLE COAL SEAMS

Estimating the potential amount of CO_2 stored in geological formations is crucial for effectively implementing CO_2 sequestration projects.[186−188] Many researchers have developed different methods to approximate the volume of CO_2 that can be stored in deep unmineable coal seams.[189−195] Several developed techniques were published in previous reviews based on experiment, volume, and simulations.[193] However, in this review section, recently developed new methods of predicting the amount of CO_2 that can be stored are analyzed.

Reference 196 developed a method to approximate the maximum amount of CO_2 stored in a Wyoming coal seam field. The established method considered gas transport within multiple radial hydraulic fractures (MRHF) and natural fractures, adsorption into the coal surface, and diffusion in the coal seam matrix. The Gaussian elimination method and Stehfest numerical inversion, the semianalytical solution based on BHP, were used to emanate a continuous line source function of coal seams to approximate the CO_2 storage capacity of the Wyoming coal field. The assumptions used during model development were the following: (1) Pressure and temperature of coal seams did not change during the injection of CO_2. (2) The flow within MRHF was not neglected. (3) The total CO_2 injection was considered constant. (4) Capillary pressure and gravity were neglected. (5) CO_2 flows within natural and hydraulic fractures obey Darcy's law, whereas flows (diffusion) in the matrix obey Fick's law, and the Langmuir isothermal drives adsorption in the coal surface. (6) Vertical wellbore MRHF solely penetrates the coal seam. The developed mathematical model to approximate maximum CO_2 storage capacity is shown in eq 19. The estimated maximum volume of the CO_2 that can be stored in the Wyoming coal seam field was 4.8×10^8 m^3.

$$Q_{\mathrm{total}} = \frac{q_{\mathrm{sc}} t_{\mathrm{D}} \chi L_{\mathrm{ref}}^2}{k_{\mathrm{fi}}} \tag{19}$$

where Q_{total} is the maximum storage capacity (m^3), q_{sc} is the injection rate at standard condition (m^3/d), t_{D} is dimensionless time (s), L_{ref} is reference length (m), and k_{fi} is initial fracture permeability (mD).

Also, ref 197 established a mathematical model to estimate the storage capacity of anthracite coal seams in the Qinshui Basin, Shanxi Province, in north China. The developed mathematical model considered three storage mechanisms: gas adsorbed in the coal matrix, free gas in the pores and fractures, and gas soluble in water. The developed mathematical model to estimate the total storage capacity is shown in eq 20. The estimated full storage capacity of CO_2 was 85.66−92.16% (adsorbed), 7.31−13.8% (free CO_2), and 0.51−0.56% (soluble CO_2).

$$M_{CO_2} = \rho_{\mathrm{g}} \times A \times H \times \rho_{\mathrm{bul}} \times (n_{\mathrm{f}} + n_{\mathrm{s}} + n_{\mathrm{ab}}) \tag{20}$$

https://doi.org/10.1021/acs.energyfuels.3c03004
Energy Fuels XXXX, XXX, XXX−XXX

Here M_{CO_2} represents the total stored gas in coal seams in tonnes, A stands for the total area of coalbed basin in m^2, H represents the thickness of coalbeds in m, ρ_{bulk} stands for bulk density of coal in g/cm^3, n_{ab} is the factor for adsorbed gas which complies with the Dubinin−Radushkevich (D−R) isotherm model in cm^3/g,[198] n_s is the factor for soluble gas in water computed from eq 21 in cm^3/g, and n_f is the factor for free gas in pores and fractures calculated from eq 22 in cm^3/g.

$$n_f = \left(\frac{\varphi(1-S_w)}{\rho_{skeletal}\rho_b^{STP}} - V_a\right)\rho_g \tag{21}$$

$$n_s = \frac{\varphi S_w S_{CO_2}}{\rho_{skeletal}} \times 22.4 \tag{22}$$

where φ is porosity, ρ_b^{STP} is the density of coal at the standard condition in g/cm^3, S_w stands for water saturation in connected fractures, V_a is sorbed phase volume, ρ_g is the density of free gas in g/cm^3, $\rho_{skeletal}$ stands for the apparent density of coal in g/cm^3, and S_{CO_2} represents the solubility of CO_2 in formation water (mol/cm^3).

Additionally, ref 199 examined the CO_2 storage capacity of anthracite coal seams collected from Qinshui Basin coal No. 3. Experiments were conducted by using two different coal samples, XJ and SH, with different characteristics under various isothermal experimental conditions to assess their theoretical CO_2 geological storage capacity (TCGSC) and effective CO_2 geologic storage capacity (ECGSC). TCGSC and ECGSC were estimated from the total stored CO_2 in 1 g of coal using eqs 23 and 24, respectively. ECGSC is multiplied with TCGSC because not all CH_4 is replaced with injected CO_2 in coal seams. The estimated CO_2 storage capacity was 9.72 gigatonnes (TCGSC) and 6.54 gigatonnes (ECGSC), in which adsorption capacity contributed more than 90% of total stored CO_2, which decreased as depth increased.

$$\text{TCGSC} = A \times H \times \rho_{coal} \times V \times \rho_g \tag{23}$$

$$\text{ECGSC} = \text{TCGSC} \times \text{RF} \tag{24}$$

where A stands for the total surface area of coal seams in m^2, ρ_{coal} represents the apparent density of coal in g/cm^3, RF represents the recovery factor for CH_4 due to CO_2 injection, H is the total height of coal in m, and ρ_g is the density of CO_2 under normal conditions. Here V is the total volume of CO_2 stored in 1 g of coal in cm^3/g and is defined in eq 25.

$$V = V_{ad} + V_{v0} + V_s \tag{25}$$

where V_{v0} is CO_2 stored in free space (nonadsorptive space) in cm^3/g for 1 g of coal, V_s is CO_2 dissolved in water (dissolution) in 1 g of coal in cm^3/g, and V_{ad} is CO_2 adsorbed in the coal surface calculated using the D−R sorption model anticipated by ref 200

In addition, ref 188 proposed a mathematical model to estimate CO_2 to be stored in uneconomical coalbeds in Alberta, Canada, under subcritical conditions. The established model assumed that the injected CO_2 replaced all the CH_4 and other gases in coal seams. The TCGSC was estimated based on CO_2 sorption isotherms measured on coal samples. The established mathematical model was based on initial gas in place (IGIP). To express the CO_2 stored in terms of mass instead of volume, the TCGSC is multiplied by the density of CO_2 of 1.873 kg/m^3. The formula to estimate TCGSC is shown in eq 26. However, it is impossible to replace all gas in the coal seams by injected CO_2; hence, the TCGSC is multiplied by the recovery factor (R_f) and completion factor to get ECGSC as expressed in eq 27. The approximated TCGSC was 20 gigatonnes, equal to 6.4 gigatonnes, after multiplying TCGSC with R_f of 0.8 and C of 0.4 for three selected coal zones. Due to the fact that only the economic zones needed to be assessed for storage capacity, it was revealed that ∼850 megatonnes of CO_2 can be stored in the Alberta coal field. The estimated global CO_2 sequestration capacity is shown in Table 9.

$$\text{TCGSC} = Ah\tilde{n}_C G_C(1 - f_a - f_m) \tag{26}$$

$$\text{ECGSC} = CR_f\text{TCGSC} \tag{27}$$

Table 9. Global CO_2 Sequestration and CH_4 Production for Coal Basins[a,b]

	estimated methane recovery (Tcm)			CO_2 storage	CO_2 storage
country	primary	ECBM	total	Tcm	Gt
United States	4.82	7.54	12.4	52.82	86.16
Canada	5.21	4.35	9.6	17.85	29.11
Mexico	0.04	0.09	0.1	0.34	0.55
total North America	10.06	111.99	22.1	71.01	115.82
Brazil	0.15	0.00	0.2	0.57	0.93
Colombia	0.10	0.22	0.3	1.29	2.11
Venezuela	0.07	0.30	0.4	3.57	5.83
total South and Central America	0.32	0.52	0.85	5.44	8.87
Czech Republic	0.06	0.00	0.1	0.00	0.00
Germany	0.45	0.00	0.5	0.62	1.01
Hungary	0.02	0.04	0.1	0.10	0.17
Kazakhstan	0.28	0.00	0.3	0.50	0.82
Poland	0.14	0.94	1.1	4.07	6.63
Russia Federation	5.66	12.61	18.3	35.20	57.41
Turkey	0.28	0.00	0.3	0.58	0.94
Ukraine	0.71	1.72	2.4	4.54	7.41
United Kingdom	0.43	1.03	1.5	2.73	4.46
Total Europe and Eurasia	8.04	16.35	24.39	48.34	78.84
Botswana	0.45	1.06	1.5	9.18	14.97
Mozambique	0.37	0.89	1.3	1.84	3.01
Namibia	0.44	1.05	1.5	2.18	3.56
South Africa	0.25	0.61	0.9	1.26	2.05
Zimbabwe	0.25	0.61	0.9	3.44	5.62
total Middle East and Africa	1.77	4.22	5.99	17.9	29.2
Australia	0.95	0.67	1.62	9.01	14.7
China	5.52	7.13	12.64	47.83	78.01
India	0.57	0.63	1.2	4.04	6.6
Indonesia	1.93	8.05	9.97	95.4	155.6
total Asia Pacific	8.96	16.47	25.43	156.28	254.91
total world	29.15	49.55	78.7	298.97	487.64

[a]Reproduced with permission from ref 201. Copyright 2014 Elsevier. [b]Tcm: trillion cubic meter; Gt: gigatonnes.

where A stands for the total area of coal seams, h represents the effective thickness of the coal seams, $\tilde{n}_C$ is bulk coal density, G_C is coal gas content, f_a is ash weight, and f_m is moisture weight content fracture.

10. CHALLENGES, RESEARCH GAPS, AND PERSPECTIVE OF STORING CO_2 SEQUESTRATION IN DEEP UNMINEABLE COAL SEAMS

Many experiments with limited simulations and pilot tests have revealed that deep unmineable coal seams have great potential to store CO_2 and recover clean energy sources (CH_4) during CO_2-ECBM technology application. Nevertheless, some challenges can hinder the technology application. The challenges encountered during CO_2 sequestration include permeability reduction; after CO_2 injection, the permeability is reduced due to coal swelling after the sorption process. The permeability reduction brings difficulty during injection by reducing the injection rate.[202,203] Also, low permeability commonly characterizes coalbeds as one of the primary factors that impede the effective injection and dispersion of carbon dioxide inside the formation.[203,204] Another is monitoring and verification; it is difficult to create efficient monitoring and verification techniques due to the complicated subsurface conditions and the requirement for long-term monitoring of CO_2 sequestration in CBM reservoirs. These factors make it difficult to evaluate the success and performance of CO_2 sequestration in CBM reservoirs.[205,206] Also, CO_2−CH_4 interactions are challenges: CO_2 and CH_4 interaction within the coal matrix can affect the sorption behavior of gases, affecting the amount of CH_4 that can be recovered and the efficiency with which CO_2 can be stored.[206−208] A further challenge is high expenses; CO_2 sequestration in CBM reservoirs incurs substantial costs, including site characterization, infrastructure development, monitoring, and operation. Assessing the project's economic feasibility is critical for its implementation.[209,210] Moreover, water saturation in coalbeds can affect CO_2 injection and migration, potentially limiting the storage capacity and the efficacy of the sequestration process.[211,212] Besides heterogeneity effects, geological diversity in CBM reservoirs, such as changes in coal properties like thickness and structure, can contribute to uneven CO_2 distribution and storage within the formation.[213,214]

Some areas that need more research toward full field operations include the following: no clear definition of unmineable coal seams suitable for CO_2 sequestration because not all coal can store CO_2. Indeterminately, more research studies need to be conducted to have assurance which coal seams are suitable for the CO_2 sequestration project to avoid CO_2 leakages in the future because coal seams are evenly distributed around the world compared to other geological options for storing CO_2. Also, deep unmineable coal seams with <1 mD permeability and depth of >1500 m are not recommended for CO_2-ECBM technology application because low permeability reduces the injection rate. Hence, to meet the minimum injection rate, it will require drilling multiple wells, which is expensive and will make a project uneconomical. Thus, more research is needed to innovate injection technology of CO_2 in coal seams with <1 mD permeability and depth of >1500 m. In addition, injection pressure and production period affect CH_4 recovery and CO_2 sequestration efficiency. In particular, early production requires a greater CO_2 injection pressure, while later prefers a lower pressure. A dynamic CO_2 injection pressure mode (for example, where the gas injection pressure is initially high before gradually lowering) may be preferable for effective CO_2 sequestration and CH_4 recovery. Thus, how to dynamically and cognitively control injection pressure to enhance CO_2 sequestration and CH_4 recovery simultaneously requires further research.

It is also important to understand the geochemical interactions between CO_2, coal, and groundwater to determine CO_2 long-term fate and potential consequences on groundwater quality, which is useful for daily life. More research is required to fully comprehend these reaction processes and their significance for CO_2 sequestration in deep unmineable coal seams. Also, more research is essential to fully understand the intricate interaction between CO_2 and CH_4 in the coal matrix, especially at the microscale level. This entails investigating the mechanisms of sorption of CH_4 in the presence of CO_2 and their effects on CO_2 sequestration and CH_4 recovery efficiencies in deep unmineable coal seams. In addition, it is essential to have a solid understanding of the long-term stability of CO_2 storage in deep unmineable coal seams. It is necessary to research the possibility of CO_2 leakage over lengthy periods. This investigation should consider geomechanical changes, geochemical processes, and CO_2 migration paths.

Addressing these challenges and research gaps requires a multifaceted, interdisciplinary approach combining geology, engineering, environmental sciences, and policy skills. Collaboration between researchers, industry, and regulatory agencies is critical for developing effective CO_2 sequestration methodologies and technologies in deep unmineable coal seams. If addressed, it will contribute to the progression and successful implementation of CO_2 sequestration toward full field application. This will result in increased storage efficiency, improved monitoring techniques, and a better understanding of the long-term impacts of CO_2 storage on the subsurface environment.

11. CONCLUSIONS

Deep unmineable coal seams have a great potential of sequestrating large amounts of CO_2 credited by impermeable caprock, which helps to prevent upward migration of CO_2, high porosity, and high carbon density, providing virtuous gas adsorption surface area for permanent CO_2 storage. Adsorption CO_2 trapping mechanisms are the dominant mechanisms in coal seams. Experiments, simulations, and pilot test applications (field application) have been carried out by different researchers to investigate the underlying mechanisms of CO_2-ECBM technology. It has been revealed that CO_2 sequestration and CH_4 production are more effective and quicker in high-rank coals than in low-rank coals. Injecting CO_2 in medium coal rank reservoirs influences CH_4 desorption, increasing CH_4 recovery. In contrast, low-rank and high-rank coals reservoirs are more favorable for CO_2 sequestration due to high micropore volume and the large specific area, which boost the CO_2 adsorption process. Furthermore, CO_2 adsorption into the coal surface increases with increasing injection pressure, enhancing CO_2 sequestration and CH_4 production. However, high injection pressure increases the operations costs. Also, from the experimental perspective, during CO_2 injection, there is competitive sorption between CO_2 and CH_4 on the surface of the coal because CO_2 has a higher affinity than CH_4 in the coal matrix. CO_2 adsorbed into the coal matrix with CH_4 desorbed enhances CO_2 sequestration and CH_4 production. The amount of CO_2 adsorbed into the coal surface is nearly twice by volume as desorbed CH_4. Apart from that, comparing the permeability of coal seams before and after Sc-CO_2 injection in unmineable coal seams revealed that Sc-CO_2 enhances coal permeability due

https://doi.org/10.1021/acs.energyfuels.3c03004
Energy Fuels XXXX, XXX, XXX−XXX

to cracks formed in pore spaces after the diffusion process into the coal surfaces.

From modeling and simulation perspectives, it was found that long-term CO_2 sequestration is better in coal seams with higher CO_2 diffusion attenuation coefficients. Also, in gas sorption models, it has been found that the D−A model is the most accurate to estimate the volume of adsorbed gas in coal seams compared to others because it may derive isotherms for any temperature employing a single isotherm, making it easier to describe injection/depletion-induced temperature change. Among the several simulators evaluated for CO_2-ECBM technology application, COMSOL, CMG-GEM, COMET3, ECLIPSE, SMED II, etc., consider several factors during CO_2 injection to imitate the field reality. COMSOL, CMG, and COMET3 simulated better CO_2 stored than other simulators. Innovating a simulator that considers all suggested CO_2 trapping mechanisms toward field application is recommended. Recently, machine learning has been applied in estimating the amount of CO_2 stored in coal seams; however, more research is recommended. In general, large volumes of CO_2 can be sequestrated in coals. If implemented successfully, more than 7.1 billion tonnes can be stored permanently in deep unmineable coal seams globally. However, storing CO_2 in deep unmineable coal seams seems uneconomical due to the high cost of capturing and separating from flue gas streams. The CH_4 produced after the CO_2-ECBM technology application helped offset some costs but did not break even due to lower gas prices and low cumulative production.

■ ASSOCIATED CONTENT

Data Availability Statement

There is no data used in this review paper.

■ AUTHOR INFORMATION

Corresponding Author

Long Yu − *School of Earth Resources, China University of Geosciences, Wuhan 430074, China;* orcid.org/0009-0007-5406-8720; Email: yulong36@cug.edu.cn

Authors

Grant Charles Mwakipunda − *School of Earth Resources, China University of Geosciences, Wuhan 430074, China;* orcid.org/0000-0003-3446-827X

Yuting Wang − *School of Earth Resources, China University of Geosciences, Wuhan 430074, China; Exploration and Development Research Institute of PetroChina Hubei Oilfield Company, Renqiu 062552, China*

Melckzedeck Michael Mgimba − *School of Earth Resources, China University of Geosciences, Wuhan 430074, China; Mbeya University of Science and Technology (MUST), Mbeya 53119, Tanzania*

Mbega Ramadhani Ngata − *School of Earth Resources, China University of Geosciences, Wuhan 430074, China;* orcid.org/0000-0002-7396-2257

Jeremiah Alhassan − *School of Earth Resources, China University of Geosciences, Wuhan 430074, China*

Christopher N. Mkono − *School of Earth Resources, China University of Geosciences, Wuhan 430074, China*

Complete contact information is available at:
https://pubs.acs.org/10.1021/acs.energyfuels.3c03004

Notes

The authors declare no competing financial interest.

Biographies

Grant Charles Mwakipunda is a Ph.D. student at China University of Geoscience (Wuhan), majoring in oil and natural gas engineering. His research interests focus on enhanced oil recovery (EOR), reservoir modeling and simulation, carbon dioxide sequestration in geological media toward decarbonization, underground hydrogen storage, and machine learning application in oil and gas engineering.

Yuting Wang is a petroleum engineer at Hubei Oilfield Company, PetroChina. She is also a Ph.D. student at the China University of Geosciences (Wuhan). Her research is focused on the formation properties characterization and recovery enhancement for coalbed methane.

Melckzedeck Michael Mgimba is a Ph.D. student at the China University of Geosciences in his fourth year and an Assistant Lecturer at Mbeya University of Science of Geoscience and Technology (MUST). Melck is an expert in Petroleum Engineering, especially on production matters. Melck is an expert on different techniques for recovering conventional and unconventional reservoirs and applying artificial intelligence (AI) to predict reservoir parameters.

Mbega Ramadhani Ngata is a researcher and Ph.D. student at the China University of Geosciences. He is researching geothermal resources, oil and gas drilling, formation damage of a reservoir, and fluid flow in porous media.

Jeremiah Alhassan is currently pursuing a Master's degree at the China University of Geosciences (Wuhan), with a specialization in oil and natural gas engineering. He is currently engaged in a research endeavor focused on reservoir geology and characterization, specifically examining fluvial sedimentary systems as a means of understanding unconventional oil and gas reserves.

Christopher N. Mkono is a Ph.D. candidate at the China University of Geosciences majoring in oil and natural gas engineering. His research area is mainly based on machine learning approaches towards source rocks potentiality, reservoir characterization, and hydrocarbon resources potential.

Long Yu is a professor in Petroleum Engineering from the China University of Geosciences (Wuhan). Dr. Yu's research interests include enhanced oil recovery and CO_2 storage in oil and gas reservoirs. His research involves the experimental and theoretical study of conformance control behavior of emulsions.

■ ACKNOWLEDGMENTS

The authors thank the Chinese Scholarship Council for their support.

■ REFERENCES

(1) Hannah, R.; Max, R.; Rosado, P. CO_2 and Greenhouse Gas Emissions. https://ourworldindata.org/co2-and-greenhouse-gas-emissions (accessed 7/29/2023).

(2) Rogelj, J. Net zero targets in science and policy. *Environ. Res. Lett.* **2023**, *18*, 021003.

(3) Mwakipunda, G. C.; Abelly, E. N.; Mgimba, M. M.; Ngata, M. R.; Nyakilla, E. E.; Yu, L. Critical Review on Carbon Dioxide Sequestration Potentiality in Methane Hydrate Reservoirs via CO_2−CH_4 Exchange: Experiments, Simulations, and Pilot Test Applications. *Energy Fuels* **2023**, *37*, 10843.

(4) Ngata, M. R.; Yang, B.; Khalid, W.; Ochilov, E.; Mwakipunda, G. C.; Aminu, M. D. Review on Experimental Investigation into Formation Damage during Geologic Carbon Sequestration: Advances and Outlook. *Energy Fuels* **2023**, *37* (9), 6382−6400.

(5) Cozzi, L.; Gould, T. World Energy Outlook 2015. *International Energy Agency*; International Energy Agency: Paris, France, 2015.

(6) Hamawand, I.; Yusaf, T.; Hamawand, S. G. Coal seam gas and associated water: A review paper. *Renewable and Sustainable Energy Reviews* **2013**, *22*, 550−560.
(7) Whitmee, S.; Anton, B.; Haines, A. Accountability for carbon emissions and health equity. *Bulletin of the World Health Organization* **2023**, *101* (2), 83−83A.
(8) United Nations Environment Programme. *Emissions gap report 2022: The closing window—Climate crisis calls for rapid transformation of societies*; UNEP: Nairobi, Kenya, 2022.
(9) Depledge, J.; Saldivia, M.; Peñasco, C. Glass half full or glass half empty?: the 2021 Glasgow Climate Conference. *Climate Policy* **2022**, *22* (2), 147−157.
(10) Mwakipunda, G. C.; Ngata, M. R.; Mgimba, M. M.; Yu, L. Carbon Dioxide Sequestration in Low Porosity and Permeability Deep Saline Aquifer: Numerical Simulation Method. *J. Energy Resour. Technol.* **2023**, *145* (7), 073401.
(11) Oelkers, E. H.; Cole, D. R. Carbon Dioxide Sequestration A Solution to a Global Problem. *Elements* **2008**, *4* (5), 305−310.
(12) Grimston, M.; Karakoussis, V.; Fouquet, R.; Van der Vorst, R.; Pearson, P.; Leach, M. The European and global potential of carbon dioxide sequestration in tackling climate change. *Climate Policy* **2001**, *1* (2), 155−171.
(13) Sahu, C.; Sircar, A.; Sangwai, J. S.; Kumar, R. Effect of methylamine, amylamine, and decylamine on the formation and dissociation kinetics of CO2 hydrate relevant for carbon dioxide sequestration. *Ind. Eng. Chem. Res.* **2022**, *61* (7), 2672−2684.
(14) Deng, Z.; Fan, S.; Wang, Y.; Lang, X.; Li, G.; Liu, F.; Li, M. High storage capacity and high formation rate of carbon dioxide hydrates via super-hydrophobic fluorinated graphenes. *Energy* **2023**, *264*, No. 126045.
(15) Keller, K.; McInerney, D.; Bradford, D. F. Carbon dioxide sequestration: how much and when? *Climatic Change* **2008**, *88*, 267−291.
(16) Liu, S.; Liu, T.; Zheng, S.; Wang, R.; Sang, S. Evaluation of carbon dioxide geological sequestration potential in coal mining area. *International Journal of Greenhouse Gas Control* **2023**, *122*, No. 103814.
(17) Zheng, J.; Chong, Z. R.; Qureshi, M. F.; Linga, P. Carbon Dioxide Sequestration via Gas Hydrates: A Potential Pathway toward Decarbonization. *Energy Fuels* **2020**, *34* (9), 10529−10546.
(18) Mazzotti, M.; Pini, R.; Storti, G.; Burlini, L. 5-Carbon dioxide (CO_2) sequestration in unmineable coal seams and use for enhanced coalbed methane recovery (ECBM). In *Developments and Innovation in Carbon Dioxide (CO_2) Capture and Storage Technology*; Maroto-Valer, M. M., Ed.; Woodhead Publishing: Cambridge, U.K., 2010; Vol. *2*, pp 127−165.
(19) Kumar, H.; Elsworth, D.; Mathews, J. P.; Liu, J.; Pone, D. Effect of CO2 injection on heterogeneously permeable coalbed reservoirs. *Fuel* **2014**, *135*, 509−521.
(20) Every, R.; Dellosso, L. New technique for removal of methane from coal. *Canadian Mining Metall. Bull.* **1972**, *65* (719), 143.
(21) Puri, R.; Yee, D. Enhanced coalbed methane recovery. In *SPE Annual Technical Conference and Exhibition, September 23−26, 1990, New Orleans, LA*; OnePetro, 1990.
(22) Gunter, W.; Gentzis, T.; Rottenfusser, B.; Richardson, R. Deep coalbed methane in Alberta, Canada: a fuel resource with the potential of zero greenhouse gas emissions. *Energy Conversion and Management* **1997**, *38*, S217−S222.
(23) Pan, Z.; Connell, L. D. Modelling permeability for coal reservoirs: a review of analytical models and testing data. *International Journal of Coal Geology* **2012**, *92*, 1−44.
(24) Mukherjee, M.; Misra, S. A review of experimental research on Enhanced Coal Bed Methane (ECBM) recovery via CO2 sequestration. *Earth-Science Reviews* **2018**, *179*, 392−410.
(25) Fulton, P. F.; Parente, C. A.; Rogers, B. A.; Shah, N.; Reznik, A. A. A Laboratory Investigation of Enhanced Recovery of Methane from Coal by Carbon Dioxide Injection. In *SPE Unconventional Gas Recovery Symposium, May 18−21, 1980, Pittsburgh, PA*; OnePetro, 1980.
(26) Zhang, C.; Wang, E.; Li, B.; Kong, X.; Xu, J.; Peng, S.; Chen, Y. Laboratory experiments of CO2-enhanced coalbed methane recovery considering CO2 sequestration in a coal seam. *Energy* **2023**, *262*, No. 125473.
(27) Zheng, S.; Yao, Y.; Sang, S.; Liu, D.; Wang, M.; Liu, S. Dynamic characterization of multiphase methane during CO2-ECBM: An NMR relaxation method. *Fuel* **2022**, *324*, No. 124526.
(28) Wong, S.; Law, D.; Deng, X.; Robinson, J.; Kadatz, B.; Gunter, W. D.; Jianping, Y.; Sanli, F.; Zhiqiang, F. Enhanced coalbed methane and CO2 storage in anthracitic coals—Micro-pilot test at South Qinshui, Shanxi, China. *International Journal of Greenhouse Gas Control* **2007**, *1* (2), 215−222.
(29) Wang, Q.; Li, W.; Zhang, D.; Wang, H.; Jiang, W.; Zhu, L.; Tao, J.; Huo, P.; Zhang, J. Influence of high-pressure CO2 exposure on adsorption kinetics of methane and CO2 on coals. *Journal of Natural Gas Science and Engineering* **2016**, *34*, 811−822.
(30) Vishal, V.; Mahanta, B.; Pradhan, S. P.; Singh, T.; Ranjith, P. Simulation of CO2 enhanced coalbed methane recovery in Jharia coalfields, India. *Energy* **2018**, *159*, 1185−1194.
(31) He, Q.; Mohaghegh, S. D.; Gholami, V. A Field Study on Simulation of Carbon Dioxide Injection and ECBM Production and Prediction of Carbon Dioxide Storage Capacity in Unmineable Coal Seam. *J. Petrol. Eng.* **2013**, *2013*, No. 803706.
(32) Robertson, E. P. Economic analysis of carbon dioxide sequestration in powder river basin coal. *International Journal of Coal Geology* **2009**, *77* (1), 234−241.
(33) Wong, S.; Gunter, W.; Mavor, M. Economics of CO_2 sequestration in coalbed methane reservoirs. In *SPE/CERI Gas Technology Symposium, April 3−5, 2000, Calgary, Alberta, Canada*; OnePetro, 2000.
(34) Hernandez, G. A.; Bello, R. O.; McVay, D. A.; Ayers, W. B.; Rushing, J. A.; Ruhl, S. K.; Hoffmann, M. F.; Ramazanova, R. I. Evaluation of the Technical and Economic Feasibility of CO_2 Sequestration and Enhanced Coalbed-Methane Recovery in Texas Low-Rank Coals. In *SPE Gas Technology Symposium, May 15−17, 2006, Calgary, Alberta, Canada*; OnePetro, 2006.
(35) IEA Greenhouse Gas R&D Programme. *Enhanced coal bed methane recovery with CO_2 sequestration*; International Energy Agency Greenhouse Gas R&D Programme: Cheltenham, U.K., 1999; Report PH3/3, p 139.
(36) Stevens, S. H.; Spector, D.; Riemer, P. Enhanced coalbed methane recovery using CO_2 injection: Worldwide resource and CO_2 sequestration potential. In *SPE International Oil and Gas Conference and Exhibition in China, November 2−6, 1998, Beijing, China*; OnePetro, 1998.
(37) Gale, J.; Freund, P. Coal-bed methane enhancement with CO2 sequestration worldwide potential. *Environmental Geosciences* **2001**, *8* (3), 210−217.
(38) Gensterblum, Y.; Merkel, A.; Busch, A.; Krooss, B. M.; Littke, R. Gas saturation and CO2 enhancement potential of coalbed methane reservoirs as a function of depthGas Saturation and CO2 Enhancement Potential of CBM Reservoirs. *Aapg Bulletin* **2014**, *98* (2), 395−420.
(39) Jia, J.; Song, H.; Jia, P. Molecular Simulation of Methane Adsorption Properties of Coal Samples with Different Coal Rank Superposition States. *ACS Omega* **2023**, *8* (3), 3461−3469.
(40) Cheng, Y.; Jiang, H.; Zhang, X.; Cui, J.; Song, C.; Li, X. Effects of coal rank on physicochemical properties of coal and on methane adsorption. *International Journal of Coal Science & Technology* **2017**, *4* (2), 129−146.
(41) Tambaria, T. N.; Sugai, Y.; Anggara, F. Experimental measurements of CO2 adsorption on Indonesian low-rank coals under various conditions. *Journal of Petroleum Exploration and Production Technology* **2023**, *13* (3), 813−826.
(42) Golding, S.; Uysal, I.; Boreham, C.; Kirste, D.; Baublys, K.; Esterle, J. Adsorption and mineral trapping dominate CO2 storage in coal systems. *Energy Procedia* **2011**, *4*, 3131−3138.
(43) Feng, Y.; Yang, W.; Chu, W. Contribution of Ash Content Related to Methane Adsorption Behaviors of Bituminous Coals. *Int. J. Chem. Eng.* **2014**, *2014*, No. 956543.

https://doi.org/10.1021/acs.energyfuels.3c03004
Energy Fuels XXXX, XXX, XXX−XXX

(44) Tambaria, T. N.; Sugai, Y.; Nguele, R. Adsorption Factors in Enhanced Coal Bed Methane Recovery: A Review. *Gases* **2022**, *2* (1), 1−21.

(45) Mallick, N.; Prabu, V. Energy analysis on Coalbed Methane (CBM) coupled power systems. *Journal of CO2 Utilization* **2017**, *19*, 16−27.

(46) Wang, H.; Ran, Q.; Liao, X.; Zhao, X.; Xu, M.; Fang, P. Study of the CO2 ECBM and sequestration in coalbed methane reservoirs with SRV. *Journal of Natural Gas Science and Engineering* **2016**, *33*, 678−686.

(47) Wolf, J.; Maaref, S.; Esmaeili, S.; Tutolo, B.; Kantzas, A. An Experimental Study on the Effects of Competitive Adsorption During Huff-N-Puff Enhanced Gas Recovery. In *SPE Canadian Energy Technology Conference and Exhibition, March 15−16, 2023, Calgary, Alberta, Canada*; OnePetro, 2023.

(48) Chatterjee, A.; Bhowmik, S.; Dutta, P. Methane/CO2 binary gas interaction on some moist, high−volatile bituminous Indian coals: 2. Pure-/mixed-gas adsorption modelling. *J. Pet. Sci. Eng.* **2022**, *208*, No. 109673.

(49) Wolf, J.; Maaref, S.; Tutolo, B.; Kantzas, A. An Experimental Study of Single Component Adsorption/Desorption Isotherms. In *SPE Canadian Energy Technology Conference, March 16−17, 2022, Calgary, Alberta, Canada*; OnePetro, 2022.

(50) Zhang, S.; Tang, S.; Li, Z.; Liu, B.; Wang, R. Effect of pore structure on competitive sorption and diffusion of mixed methane and carbon dioxide in anthracite, South Qinshui Basin, China. *International Journal of Coal Geology* **2022**, *253*, No. 103956.

(51) Mahanta, B.; Vishal, V. CO_2 Sequestration and Enhanced Coalbed Methane Recovery: Worldwide Status and Indian Scenario. In *Applied Geology: Approaches to Future Resource Management*; De Maio, M., Tiwari, A. K., Eds.; Springer International Publishing: Cham, 2020; pp 161−181.

(52) Mazumder, S.; van Hemert, P.; Busch, A.; Wolf, K. H. A. A.; Tejera-Cuesta, P. Flue gas and pure CO2 sorption properties of coal: A comparative study. *International Journal of Coal Geology* **2006**, *67* (4), 267−279.

(53) Gan, H.; Nandi, S. P.; Walker, P. L. Nature of the porosity in American coals. *Fuel* **1972**, *51* (4), 272−277.

(54) Bai, G.; Zhou, Z.; Li, X.; Cheng, Y.; Hu, K.; Chen, Y.; Zhou, X. Quantitative analysis of carbon dioxide replacement of adsorbed methane in different coal ranks using low-field NMR technique. *Fuel* **2022**, *326*, No. 124980.

(55) Talapatra, A. A study on the carbon dioxide injection into coal seam aiming at enhancing coal bed methane (ECBM) recovery. *Journal of Petroleum Exploration and Production Technology* **2020**, *10* (5), 1965−1981.

(56) Gonzalez, R.; Schepers, K.; Riestenberg, D.; Koperna, G.; Oudinot, A. Assessment of the potential and economic performance for ECBM recovery and CO_2 sequestration. In *Latin American and Caribbean Petroleum Engineering Conference, May 31−June 30, 2009, Cartagena de Indias, Colombia*; OnePetro, 2009.

(57) Liu, L.; Jin, C.; Li, L.; Xu, C.; Sun, P.; Meng, Z.; An, L. Coalbed methane adsorption capacity related to maceral compositions. *Energy Exploration & Exploitation* **2020**, *38* (1), 79−91.

(58) Huang, L.; Ning, Z.; Wang, Q.; Zhang, W.; Cheng, Z.; Wu, X.; Qin, H. Effect of organic type and moisture on CO2/CH4 competitive adsorption in kerogen with implications for CO2 sequestration and enhanced CH4 recovery. *Applied Energy* **2018**, *210*, 28−43.

(59) Kim, A. G. *Estimating methane content of bituminous coalbeds from adsorption data*; Department of the Interior, Bureau of Mines: Pittsburgh, PA, 1977; Report 8245.

(60) Gao, Z.; Ma, D.; Chen, Y.; Zheng, C.; Teng, J. Study for the Effect of Temperature on Methane Desorption Based on Thermodynamics and Kinetics. *ACS Omega* **2021**, *6* (1), 702−714.

(61) Mohanty, M. M.; Pal, B. K. Sorption behavior of coal for implication in coal bed methane an overview. *International Journal of Mining Science and Technology* **2017**, *27* (2), 307−314.

(62) Zeng, F.; Peng, F.; Guo, J.; Wang, D.; Zhang, S.; Zhang, P.; Zhang, B. Gas transport study in the confined microfractures of coal reservoirs. *Journal of Natural Gas Science and Engineering* **2019**, *68*, No. 102920.

(63) Zimmerman, R. W.; Chen, G.; Hadgu, T.; Bodvarsson, G. S. A numerical dual-porosity model with semianalytical treatment of fracture/matrix flow. *Water Resour. Res.* **1993**, *29* (7), 2127−2137.

(64) Crank, J. *The mathematics of diffusion*; Oxford University Press: Oxford, 1979.

(65) Wang, K.; Wang, Y.; Guo, H.; Zhang, J.; Zhang, G. Modelling of multiple gas transport mechanisms through coal particle considering thermal effects. *Fuel* **2021**, *295*, No. 120587.

(66) Busch, A.; Gensterblum, Y. CBM and CO2-ECBM related sorption processes in coal: a review. *International Journal of Coal Geology* **2011**, *87* (2), 49−71.

(67) Busch, A.; Gensterblum, Y.; Krooss, B. M.; Littke, R. Methane and carbon dioxide adsorption−diffusion experiments on coal: upscaling and modeling. *International Journal of Coal Geology* **2004**, *60* (2), 151−168.

(68) Fan, C.; Elsworth, D.; Li, S.; Chen, Z.; Luo, M.; Song, Y.; Zhang, H. Modelling and optimization of enhanced coalbed methane recovery using CO2/N2 mixtures. *Fuel* **2019**, *253*, 1114−1129.

(69) Gale, J. J., Using coal seams for CO_2 sequestration. *Geol. Belg.* **2004**.73-4.

(70) Dutka, B.; Kudasik, M.; Pokryszka, Z.; Skoczylas, N.; Topolnicki, J.; Wierzbicki, M. Balance of CO2/CH4 exchange sorption in a coal briquette. *Fuel Process. Technol.* **2013**, *106*, 95−101.

(71) Busch, A.; Gensterblum, Y.; Krooss, B. M.; Siemons, N. Investigation of high-pressure selective adsorption/desorption behaviour of CO2 and CH4 on coals: An experimental study. *International Journal of Coal Geology* **2006**, *66* (1), 53−68.

(72) Yu, H.; Yuan, J.; Guo, W.; Cheng, J.; Hu, Q. A preliminary laboratory experiment on coalbed methane displacement with carbon dioxide injection. *International Journal of Coal Geology* **2008**, *73* (2), 156−166.

(73) Ceglarska-Stefańska, G.; Zarębska, K. The competitive sorption of CO2 and CH4 with regard to the release of methane from coal. *Fuel Process. Technol.* **2002**, *77−78*, 423−429.

(74) Yao, H.; Chen, Y.; Liang, W.; Song, X. Experimental study on temperature change caused by ScCO2 adsorption−desorption during carbon sequestration in deep coal seam. *Fuel* **2023**, *339*, No. 127408.

(75) Pan, Z.; Ye, J.; Zhou, F.; Tan, Y.; Connell, L. D.; Fan, J. CO2 storage in coal to enhance coalbed methane recovery: a review of field experiments in China. *International Geology Review* **2018**, *60* (5−6), 754−776.

(76) Li, Y.; Tang, D.; Xu, H.; Meng, Y.; Li, J. Experimental research on coal permeability: the roles of effective stress and gas slippage. *Journal of Natural Gas Science and Engineering* **2014**, *21*, 481−488.

(77) Topolnicki, J.; Kudasik, M.; Dutka, B. Simplified model of the CO2/CH4 exchange sorption process. *Fuel Process. Technol.* **2013**, *113*, 67−74.

(78) Shi, J. Q.; Durucan, S. A bidisperse pore diffusion model for methane displacement desorption in coal by CO2 injection☆. *Fuel* **2003**, *82* (10), 1219−1229.

(79) Wang, F. Y.; Zhu, Z. H.; Massarotto, P.; Rudolph, V. Mass transfer in coal seams for CO2 sequestration. *AIChE J.* **2007**, *53* (4), 1028−1049.

(80) Seto, C. J.; Jessen, K.; Orr, F. M. A Four-Component, Two-Phase Flow Model for CO_2 Storage and Enhanced Coalbed Methane Recovery. In *SPE Annual Technical Conference and Exhibition, September 24−27, 2006, San Antonio, TX*; OnePetro, 2006.

(81) Pini, R.; Storti, G.; Mazzotti, M. A model for enhanced coal bed methane recovery aimed at carbon dioxide storage. *Adsorption* **2011**, *17* (5), 889−900.

(82) Mazumder, S.; Karnik, A.; Wolf, K. H. Swelling of Coal in Response to CO2 Sequestration for ECBM and Its Effect on Fracture Permeability. *SPE Journal* **2006**, *11* (03), 390−398.

(83) Pajdak, A.; Kudasik, M.; Skoczylas, N.; Wierzbicki, M.; Teixeira Palla Braga, L. Studies on the competitive sorption of CO2 and CH4 on hard coal. *International Journal of Greenhouse Gas Control* **2019**, *90*, No. 102789.

https://doi.org/10.1021/acs.energyfuels.3c03004
Energy Fuels XXXX, XXX, XXX−XXX

(84) Krooss, B. M.; van Bergen, F.; Gensterblum, Y.; Siemons, N.; Pagnier, H. J. M.; David, P. High-pressure methane and carbon dioxide adsorption on dry and moisture-equilibrated Pennsylvanian coals. *International Journal of Coal Geology* **2002**, *51* (2), 69−92.
(85) Li, X.; Fu, X.; Ranjith, P.; Fang, Y. Retained water content after nitrogen driving water on flooding saturated high volatile bituminous coal using low-field nuclear magnetic resonance. *Journal of Natural Gas Science and Engineering* **2018**, *57*, 189−202.
(86) Wei, G.; Wen, H.; Deng, J.; Ma, L.; Li, Z.; Lei, C.; Fan, S.; Liu, Y. Liquid CO2 injection to enhance coalbed methane recovery: An experiment and in-situ application test. *Fuel* **2021**, *284*, No. 119043.
(87) Arif, M.; Barifcani, A.; Lebedev, M.; Iglauer, S. CO2-wettability of low to high rank coal seams: Implications for carbon sequestration and enhanced methane recovery. *Fuel* **2016**, *181*, 680−689.
(88) Ibrahim, A. F.; Nasr-El-Din, H. A. CO_2 Sequestration in Unmineable Coal Seams. In *SPE/IATMI Asia Pacific Oil & Gas Conference and Exhibition, Nusa Dua, Bali, Indonesia, October 20−22, 2015*; OnePetro, 2015.
(89) Ghosh, S.; Adsul, T.; Varma, A. K. Organic matter and mineralogical acumens in CO2 sequestration. *Green Sustainable Process for Chemical and Environmental Engineering and Science* **2023**, 561−594.
(90) Al Hameli, F.; Belhaj, H.; Al Dhuhoori, M. CO2 Sequestration Overview in Geological Formations: Trapping Mechanisms Matrix Assessment. *Energies* **2022**, *15* (20), 7805.
(91) Liu, X.; Wu, C.; Zhao, K. Feasibility and Applicability Analysis of CO2-ECBM Technology Based on CO2−H2O−Coal Interactions. *Energy Fuels* **2017**, *31* (9), 9268−9274.
(92) Pearce, J.; Raza, S.; Baublys, K.; Hayes, P.; Firouzi, M.; Rudolph, V. Unconventional CO2 Storage: CO2 mineral Trapping Predicted in Characterized Shales, Sandstones, and Coal Seam Interburden. *SPE Journal* **2022**, *27* (05), 3218−3239.
(93) Zhang, X.; Ranjith, P. G. Experimental investigation of effects of CO2 injection on enhanced methane recovery in coal seam reservoirs. *Journal of CO2 Utilization* **2019**, *33*, 394−404.
(94) Prusty, B.; Harpalani, S. A Laboratory study of methane/CO_2 exchange in an enhanced CBM recovery scenario. In *2004 International Coalbed Methane Symposium*; University of Alabama: Tuscaloosa, AL, 2004; pp 12−14.
(95) Hadi Mosleh, M.; Sedighi, M.; Vardon, P. J.; Turner, M. Efficiency of Carbon Dioxide Storage and Enhanced Methane Recovery in a High Rank Coal. *Energy Fuels* **2017**, *31* (12), 13892−13900.
(96) Prusty, B. K. Sorption of methane and CO2 for enhanced coalbed methane recovery and carbon dioxide sequestration. *Journal of Natural Gas Chemistry* **2008**, *17* (1), 29−38.
(97) Han, S.; Sang, S.; Liang, J.; Zhang, J. Supercritical CO 2 adsorption in a simulated deep coal reservoir environment, implications for geological storage of CO 2 in deep coals in the southern Qinshui Basin, China. *Energy Science & Engineering* **2019**, *7* (2), 488−503.
(98) Li, X.; Yu, H.; Lebedev, M.; Lu, M.; Yuan, Y.; Yang, Z.; Cheng, W.; Chen, S.; Zhan, J.; Ding, S.; Johnson, L. The Influence of CO2 Saturated Brine on Microstructure of Coal: Implications for Carbon Geo-Sequestration. *Front. Energy Res.* **2022**, *10*, 11.
(99) Fu, Z.; Jia, B.; Wang, Y.; Tian, W. Experimental Study on the Effect of CO2 Injection Pressure on the Migration Characteristics and Extraction Effects of Replacement CH4. *ACS Omega* **2023**, *8* (31), 28583−28591.
(100) Ma, T.; Rutqvist, J.; Liu, W.; Zhu, L.; Kim, K. Modeling of CO2 sequestration in coal seams: Role of CO2-induced coal softening on injectivity, storage efficiency and caprock deformation. *Greenhouse Gases: Science and Technology* **2017**, *7* (3), 562−578.
(101) Qiao, L.; Deng, C.; Fan, Y. Numerical simulation study on CO2 storage in coalbed. *Energy Sources, Part A: Recovery, Utilization, and Environmental Effects* **2020**, *42* (4), 446−459.
(102) Wang, L.; Wang, Z.; Li, K.; Chen, H. Comparison of enhanced coalbed methane recovery by pure N2 and CO2 injection: Experimental observations and numerical simulation. *Journal of Natural Gas Science and Engineering* **2015**, *23*, 363−372.
(103) Fan, Y.; Deng, C.; Zhang, X.; Li, F.; Wang, X.; Qiao, L. Numerical study of CO2-enhanced coalbed methane recovery. *International Journal of Greenhouse Gas Control* **2018**, *76*, 12−23.
(104) Zhu, W.; Wei, C.; Liu, J.; Xu, T.; Elsworth, D. Impact of gas adsorption induced coal matrix damage on the evolution of coal permeability. *Rock mechanics and rock engineering* **2013**, *46*, 1353−1366.
(105) Zhao, L.; Guanhua, N.; Yongzan, W.; Hehe, J.; Yixin, L.; Qiming, H.; Wanpeng, H. Analysis of permeability evolution mechanism during CO2 enhanced coalbed methane recovery based on impact factor method. *Fuel* **2021**, *304*, No. 121389.
(106) Qu, H.; Liu, J.; Chen, Z.; Wang, J.; Pan, Z.; Connell, L.; Elsworth, D. Complex evolution of coal permeability during CO2 injection under variable temperatures. *International Journal of Greenhouse Gas Control* **2012**, *9*, 281−293.
(107) Chen, Z.; Liu, J.; Elsworth, D.; Connell, L. D.; Pan, Z. Impact of CO2 injection and differential deformation on CO2 injectivity under in-situ stress conditions. *International Journal of Coal Geology* **2010**, *81* (2), 97−108.
(108) Kong, X.; Wang, E.; Liu, Q.; Li, Z.; Li, D.; Cao, Z.; Niu, Y. Dynamic permeability and porosity evolution of coal seam rich in CBM based on the flow-solid coupling theory. *Journal of Natural Gas Science and Engineering* **2017**, *40*, 61−71.
(109) Yang, R.; Liu, W.; Ma, T.; Xie, J.; Hu, Y.; Zhou, R.; Yang, Y. A Fully Coupled Hydromechanical Model for CO2 Sequestration in Coal Seam: the Roles of Multiphase Flow and Gas Dynamic Diffusion on Fluid Transfer and Coal Behavior. *Geofluids* **2020**, *2020*, 1−14.
(110) Li, S.; Fan, C.; Han, J.; Luo, M.; Yang, Z.; Bi, H. A fully coupled thermal-hydraulic-mechanical model with two-phase flow for coalbed methane extraction. *Journal of Natural Gas Science and Engineering* **2016**, *33*, 324−336.
(111) Liu, T.; Lin, B.; Yang, W.; Liu, T.; Kong, J.; Huang, Z.; Wang, R.; Zhao, Y. Dynamic diffusion-based multifield coupling model for gas drainage. *Journal of Natural Gas Science and Engineering* **2017**, *44*, 233−249.
(112) Thararoop, P.; Karpyn, Z. T.; Ertekin, T. Development of a multi-mechanistic, dual-porosity, dual-permeability, numerical flow model for coalbed methane reservoirs. *Journal of Natural Gas Science and Engineering* **2012**, *8*, 121−131.
(113) Zhu, W.; Wei, C.; Liu, J.; Qu, H.; Elsworth, D. A model of coal−gas interaction under variable temperatures. *International Journal of Coal Geology* **2011**, *86* (2−3), 213−221.
(114) Fan, N.; Wang, J.; Deng, C.; Fan, Y.; Mu, Y.; Wang, T. Numerical study on enhancing coalbed methane recovery by injecting N2/CO2 mixtures and its geological significance. *Energy Science & Engineering* **2020**, *8* (4), 1104−1119.
(115) Teng, T.; Wang, Y.; He, X.; Chen, P. Mathematical modeling and simulation on the stimulation interactions in coalbed methane thermal recovery. *Processes* **2019**, *7* (8), 526.
(116) Sun, X.; Zhang, Y.; Li, K.; Gai, Z. A new mathematical simulation model for gas injection enhanced coalbed methane recovery. *Fuel* **2016**, *183*, 478−488.
(117) Fan, Z.; Fan, G.; Zhang, D.; Zhang, L.; Zhang, S.; Liang, S.; Yu, W. Optimal injection timing and gas mixture proportion for enhancing coalbed methane recovery. *Energy* **2021**, *222*, No. 119880.
(118) Yamaguchi, S.; Ohga, K.; Fujioka, M.; Muto, S. Prospect of CO_2 sequestration in the Ishikari Coal Field, Japan. In *Greenhouse Gas Control Technologies 7*; Rubin, E. S., Keith, D. W., Gilboy, C. F., Wilson, M., Morris, T., Gale, J., Thambimuthu, K., Eds.; Elsevier Science Ltd.: Oxford, 2005; pp 423−430.
(119) Clarkson, C. *The Allison Unit CO_2−ECBM Pilot: A Reservoir Modeling Study*; U.S. Department of Energy: Washington, D.C., 2003.
(120) Kronimus, A.; Busch, A.; Alles, S.; Juch, D.; Jurisch, A.; Littke, R. A preliminary evaluation of the CO2 storage potential in unminable coal seams of the Münster Cretaceous Basin, Germany. *International Journal of Greenhouse Gas Control* **2008**, *2* (3), 329−341.
(121) Ross, H. E.; Hagin, P.; Zoback, M. D. CO2 storage and enhanced coalbed methane recovery: Reservoir characterization and fluid flow simulations of the Big George coal, Powder River Basin,

Wyoming, USA. *International Journal of Greenhouse Gas Control* **2009**, *3* (6), 773−786.

(122) Wang, Z.; Sang, S.; Zhou, X.; Liu, X. Numerical study on CO2 sequestration in low-permeability coal reservoirs to enhance CH4 recovery: Gas driving water and staged inhibition on CH4 output. *J. Pet. Sci. Eng.* **2022**, *214*, No. 110478.

(123) Ridha, S.; Pratama, E.; Ismail, M. Performance assessment of CO2 sequestration in a horizontal well for enhanced coalbed methane recovery in deep unmineable coal seams. *Chem. Eng. Trans.* **2017**, *56*, 589−594.

(124) Dutta, P.; Harpalani, S.; Prusty, B. Modeling of CO2 sorption on coal. *Fuel* **2008**, *87* (10), 2023−2036.

(125) Langmuir, I. The constitution and fundamental properties of solids and liquids. Part I. Solids. *Journal of the American chemical society* **1916**, *38* (11), 2221−2295.

(126) Brunauer, S.; Emmett, P. H.; Teller, E. Adsorption of gases in multimolecular layers. *Journal of the American chemical society* **1938**, *60* (2), 309−319.

(127) Bering, B.; Dubinin, M.; Serpinsky, V. On thermodynamics of adsorption in micropores. *J. Colloid Interface Sci.* **1972**, *38* (1), 185−194.

(128) Amankwah, K.; Schwarz, J. A modified approach for estimating pseudo-vapor pressures in the application of the Dubinin-Astakhov equation. *Carbon* **1995**, *33* (9), 1313−1319.

(129) Myers, A. L.; Prausnitz, J. M. Thermodynamics of mixed-gas adsorption. *AIChE J.* **1965**, *11* (1), 121−127.

(130) Weniger, P.; Franců, J.; Hemza, P.; Krooss, B. M. Investigations on the methane and carbon dioxide sorption capacity of coals from the SW Upper Silesian Coal Basin, Czech Republic. *International Journal of Coal Geology* **2012**, *93*, 23−39.

(131) Dubinin, M.; Astakhov, V.; Izv. Development of the concepts of volume filling of micropores in the adsorption of gases and vapors by microporous adsorbents. *Akad. Nauk SSSR, Ser. Khim. (Engl. Transl.)* **1971**, *20*, 3.

(132) Merkel, A.; Gensterblum, Y.; Krooss, B. M.; Amann, A. Competitive sorption of CH4, CO2 and H2O on natural coals of different rank. *International Journal of Coal Geology* **2015**, *150*, 181−192.

(133) Locke, J. E.; Winschel, R. A.; Bajura, R.; Wilson, T.; Siriwardane, H.; Rauch, H.; Mohaghegh, S. CO_2 sequestration in unmineable coal with enhanced coal bed methane recovery (The Marshall County Project). In *Proceedings of the 2011 International Pittsburgh Coal Conference*; Curran Associates, Inc.: Pittsburgh, PA, 2011.

(134) Fujioka, M.; Yamaguchi, S.; Nako, M. CO2-ECBM field tests in the Ishikari Coal Basin of Japan. *International Journal of Coal Geology* **2010**, *82* (3−4), 287−298.

(135) Yamaguchi, S.; Ohga, K.; Fujioka, M.; Nako, M. Field test and history matching of the CO2 sequestration project in coal seams in Japan. *International Journal of the Society of Materials Engineering for Resources* **2006**, *13* (2), 64−69.

(136) Yamaguchi, S.; Ohga, K.; Fujioka, M.; Muto, S. Prospect of CO_2 sequestration in the Ishikari coal field, Japan. In *Greenhouse Gas Control Technologies 7*; Elsevier: Oxford, 2005; pp 423−430.

(137) Kelafant, J.; Stevens, S.; Boyer, I. Vast resource potential exists in many countries. *Oil Gas J. (United States)* **1992**, *90* (44).

(138) Mavor, M. J.; Gunter, W. D.; Robinson, J. R. Alberta Multiwell Micro-Pilot Testing for CBM Properties, Enhanced Methane Recovery and CO_2 Storage Potential. In *SPE Annual Technical Conference and Exhibition, September 26−29, 2004, Houston, TX*; 2004.

(139) Connell, L.; Pan, Z.; Camilleri, M.; Meng, S.; Down, D.; Carras, J.; Zhang, W.; Fu, X.; Guo, B.; Briggs, C.; Lupton, N. Description of a CO2 enhanced coal bed methane field trial using a multi-lateral horizontal well. *International Journal of Greenhouse Gas Control* **2014**, *26*, 204−219.

(140) Ye, J.; Zhang, B.; Sam, W. Test of and evaluation on elevation of coalbed methane recovery ratio by injecting and burying CO2 for 3# coal seam of north section of Shizhuang, Qingshui Basin, Shanxi. *Chin. Acad. Eng.* **2012**, *14* (2), 38−44.

(141) Ye, J.; Zhang, B. *Deep coal reservoir CO_2 ECBM research and equipment development: Final Report−National Science and Technology major projects* (in Chinese); China United Coalbed Methane Corp., 2016.

(142) Oudinot, A. Y.; Koperna, G. J.; Philip, Z. G.; Liu, N.; Heath, J. E.; Wells, A.; Young, G. B.; Wilson, T. CO2 injection performance in the Fruitland coal fairway, San Juan Basin: results of a field pilot. *SPE Journal* **2011**, *16* (04), 864−879.

(143) Frailey, S.; Parris, T.; Damico, J.; Okwen, R.; McKaskle, R.; Monson, C.; Goodwin, J.; Beck, E.; Berger, P.; Butsch, R. *Sequestration and enhanced coal bed methane: Tanquary Farms test site, Wabash County, Illinois*; University of Illinois at Urbana−Champaign,: Urbana−Champaign, IL, 2012.

(144) Finley, R. *An Assessment of Geological Carbon Storage Options in the Illinois Basin: Validation Phase*; University of Illinois at Urbana−Champaign: Urbana−Champaign, IL, 2012.

(145) Ripepi, N. Central Appalachian Basin ECBM field projects: Results and future plans. In *8th International Forum on Geologic Sequestration of CO_2 in Coal Seams and Gas Shale Reservoirs "Coal-Seq VIII" and "Shale-Seq I", October 23−24, 2012*; 2012; p 24.

(146) Karmis, M.; Ripepi, N.; Gilliland, E.; Louk, A.; Tang, X.; Keles, C.; Schlosser, C.; Diminick, E.; McClure, M.; Hill, G. *Central Appalachian Basin Unconventional (Coal/Organic Shale) Reservoir Small Scale CO_2 Injection Test*; Virginia Polytechnic Institute and State University (Virginia Tech): Blacksburg, VA, 2018.

(147) Pashin, J. C.; Clark, P. E.; McIntyre-Redden, M. R.; Carroll, R. E.; Esposito, R. A.; Oudinot, A. Y.; Koperna, G. J., Jr SECARB CO2 injection test in mature coalbed methane reservoirs of the Black Warrior Basin, Blue Creek Field, Alabama. *International Journal of Coal Geology* **2015**, *144*, 71−87.

(148) Pagnier, H.; van Bergen, F.; Krzystolik, P.; Skiba, J.; Jura, B.; Hadro, J.; Wentink, P.; De-Smedt, G.; Kretzschmar, H.-J.; Fröbel, J.; et al. Field experiment of ECBM-CO_2 in the Upper Silesian Basin of Poland (RECOPOL). In *Greenhouse Gas Control Technologies 7*; Rubin, E. S., Keith, D. W., Gilboy, C. F., Wilson, M., Morris, T., Gale, J., Thambimuthu, K., Eds.; Elsevier Science Ltd.: Oxford, 2005; pp 1391−1397.

(149) van Bergen, F.; Krzystolik, P.; van Wageningen, N.; Pagnier, H.; Jura, B.; Skiba, J.; Winthaegen, P.; Kobiela, Z. Production of gas from coal seams in the Upper Silesian Coal Basin in Poland in the post-injection period of an ECBM pilot site. *International Journal of Coal Geology* **2009**, *77* (1), 175−187.

(150) Yang, Y.; Clarkson, C. R.; Hamdi, H.; Ghanizadeh, A.; Blinderman, M. S.; Evans, C. Field pilot testing and reservoir simulation to evaluate processes controlling CO2 injection and associated in-situ fluid migration in deep coal. *International Journal of Coal Geology* **2023**, *275*, No. 104317.

(151) Masum, S.; Thomas, H.; Stańczyk, K.; Kempka, T.; Bezak, B.; Kapusta, K.; Otto, C.; Nakaten, N.; Chen, M.; Sadasivam, S. The Comprehensive Overview of the ROCCS Project. https://roccsproject.com/dissemination (accessed 07/17/2023).

(152) Gal, F.; Proust, E.; Leynet, A. CO2 Injection in a Coal Seam − Insights from the European Carbolab Project with Focus on Water Geochemical Monitoring. *Energy Procedia* **2014**, *63*, 5836−5848.

(153) Sakurovs, R.; Lavrencic, S. Contact angles in CO2-water-coal systems at elevated pressures. *International Journal of Coal Geology* **2011**, *87* (1), 26−32.

(154) Chaturvedi, T.; Schembre, J. M.; Kovscek, A. R. Spontaneous imbibition and wettability characteristics of Powder River Basin coal. *International Journal of Coal Geology* **2009**, *77* (1), 34−42.

(155) Shojai Kaveh, N.; Rudolph, E. S. J.; Wolf, K.-H. A. A.; Ashrafizadeh, S. N. Wettability determination by contact angle measurements: hvbB coal−water system with injection of synthetic flue gas and CO2. *J. Colloid Interface Sci.* **2011**, *364* (1), 237−247.

(156) Saghafi, A.; Pinetown, K. L.; Javanmard, H. *Gas Wettability of Coal and Implications for Gas Desorption and Drainage*; University of Wollongong: Wollongong, Australia, 2014..

https://doi.org/10.1021/acs.energyfuels.3c03004
Energy Fuels XXXX, XXX, XXX−XXX

(157) Plug, W.-J.; Mazumder, S.; Bruining, J. Capillary Pressure and Wettability Behavior of CO2 Sequestration in Coal at Elevated Pressures. *SPE Journal* **2008**, *13* (04), 455−464.

(158) Mazumder, S.; Plug, W.-J.; Bruining, H. Capillary Pressure and Wettability Behavior of Coal−Water−Carbon Dioxide System. In *SPE Annual Technical Conference and Exhibition, October 5−8, 2003, Denver, CO*; OnePetro, 2003.

(159) Zheng, S.; Yao, Y.; Elsworth, D.; Liu, D.; Cai, Y. Dynamic Fluid Interactions during CO2-Enhanced Coalbed Methane and CO2 Sequestration in Coal Seams. Part 1: CO2−CH4 Interactions. *Energy Fuels* **2020**, *34* (7), 8274−8282.

(160) Zheng, S.; Yao, Y.; Elsworth, D.; Liu, D.; Cai, Y. Dynamic fluid interactions during CO2-ECBM and CO2 sequestration in coal seams. Part 2: CO2-H2O wettability. *Fuel* **2020**, *279*, No. 118560.

(161) Zhu, C.; Wan, J.; Tokunaga, T. K.; Liu, N.; Lin, B.; Wu, H. Impact of CO2 injection on wettability of coal at elevated pressure and temperature. *International Journal of Greenhouse Gas Control* **2019**, *91*, No. 102840.

(162) Al-Yaseri, A. Z.; Roshan, H.; Xu, X.; Zhang, Y.; Sarmadivaleh, M.; Lebedev, M.; Barifcani, A.; Iglauer, S. Coal Wettability After CO2 Injection. *Energy Fuels* **2017**, *31* (11), 12376−12382.

(163) Shojai Kaveh, N.; Wolf, K. H.; Ashrafizadeh, S. N.; Rudolph, E. S. J. Effect of coal petrology and pressure on wetting properties of wet coal for CO2 and flue gas storage. *International Journal of Greenhouse Gas Control* **2012**, *11*, S91−S101.

(164) Saghafi, A.; Javanmard, H.; Pinetown, K. Study of coal gas wettability for CO 2 storage and CH 4 recovery. *Geofluids* **2014**, *14* (3), 310−325.

(165) Bishara, D.; Xie, Y.; Liu, W. K.; Li, S. A state-of-the-art review on machine learning-based multiscale modeling, simulation, homogenization and design of materials. *Archives of computational methods in engineering* **2023**, *30* (1), 191−222.

(166) Liang, B.; Liu, J.; You, J.; Jia, J.; Pan, Y.; Jeong, H. Hydrocarbon production dynamics forecasting using machine learning: A state-of-the-art review. *Fuel* **2023**, *337*, No. 127067.

(167) Wang, H.; Chen, S. Insights into the Application of Machine Learning in Reservoir Engineering: Current Developments and Future Trends. *Energies* **2023**, *16* (3), 1392.

(168) Yuan, J.; Mao, W.; Hu, C.; Zheng, J.; Zheng, D.; Yang, Y. Leak detection and localization techniques in oil and gas pipeline: A bibliometric and systematic review. *Engineering Failure Analysis* **2023**, *146*, No. 107060.

(169) Soomro, A. A.; Mokhtar, A. A.; Kurnia, J. C.; Lashari, N.; Lu, H.; Sambo, C. Integrity assessment of corroded oil and gas pipelines using machine learning: A systematic review. *Engineering Failure Analysis* **2022**, *131*, No. 105810.

(170) Zhong, R.; Salehi, C.; Johnson, R., Jr Machine learning for drilling applications: A review. *Journal of Natural Gas Science and Engineering* **2022**, *108*, No. 104807.

(171) Zhong, R. Using Machine Learning to Improve Drilling of Unconventional Resources. In *Machine Learning Applications in Subsurface Energy Resource Management*; CRC Press: Boca Raton, FL, 2022; pp 91−110.

(172) Ibrahim, A. F. Prediction of coal wettability using machine learning for the application of CO2 sequestration. *International Journal of Greenhouse Gas Control* **2022**, *118*, No. 103670.

(173) Ibrahim, A. F. Application of various machine learning techniques in predicting coal wettability for CO2 sequestration purpose. *International Journal of Coal Geology* **2022**, *252*, No. 103951.

(174) Ibrahim, A. F. Robust Models to Predict Coal Wettability for CO_2 Sequestration Applications. In *Offshore Technology Conference, May 2−5, 2022, Houston, TX*; OnePetro, 2022.

(175) Giraldo, L. J.; Medina, O. E.; Ortiz-Pérez, V.; Franco, C. A.; Cortés, F. B. Enhanced Carbon Storage Process from Flue Gas Streams Using Rice Husk Silica Nanoparticles: An Approach in Shallow Coal Bed Methane Reservoirs. *Energy Fuels* **2023**, 37 (4), 2945−2959.

(176) Rodriguez Acevedo, E.; Cortés, F. B.; Franco, C. A.; Carrasco-Marín, F.; Pérez-Cadenas, A. F.; Fierro, V.; Celzard, A.; Schaefer, S.; Cardona Molina, A. An Enhanced Carbon Capture and Storage Process (e-CCS) Applied to Shallow Reservoirs Using Nanofluids Based on Nitrogen-Rich Carbon Nanospheres. *Materials* **2019**, *12* (13), 2088.

(177) Rodriguez Acevedo, E.; Franco, C. A.; Carrasco-Marín, F.; Pérez-Cadenas, A. F.; Cortés, F. B. Biomass-Derived Carbon Molecular Sieves Applied to an Enhanced Carbon Capture and Storage Process (e-CCS) for Flue Gas Streams in Shallow Reservoirs. *Nanomaterials* **2020**, *10* (5), 980.

(178) Boonpoke, A.; Chiarakorn, S.; Laosiripojana, N.; Chidthaisong, A. Enhancement of carbon dioxide capture by amine-modified rice husk mesoporous material. *Environmental Progress & Sustainable Energy* **2016**, *35* (6), 1716−1723.

(179) Li, X.; Wang, Z.; Liu, Z.; Feng, R.; Song, S.; Huang, J.; Fang, Y. A novel preparation of solid amine sorbents for enhancing CO2 adsorption capacity using alumina-extracted waste. *Energy* **2022**, *248*, No. 123677.

(180) Liu, H.; Wang, S.; Wang, X.; Feng, X.; Chen, S. A stable solid amine adsorbent with interconnected open-cell structure for rapid CO2 adsorption and CO2/CH4 separation. *Energy* **2022**, *258*, No. 124899.

(181) Tan, M.; Li, X.; Feng, Y.; Wang, B.; Han, L.; Bao, W.; Chang, L.; Wang, J. Fly ash-derived mesoporous silica with large pore volume for augmented CO2 capture. *Fuel* **2023**, *351*, No. 128874.

(182) Li, N.; Feng, W.; Yu, J.; Chen, F.; Zhang, Q.; Zhu, S.; Hu, Y.; Li, Y. Recent Advances in Geological Storage: Trapping Mechanisms, Storage Sites, Projects, and Application of Machine Learning. *Energy Fuels* **2023**, *37* (14), 10087−10111.

(183) Medina, O. E.; Moncayo-Riascos, I.; Franco, C. A.; Cortés, F. B. Molecular Dynamic Simulation and Experiments on n-C7 Asphaltene Pyrolysis under High-Pressure Conditions Using Ceria-Based Nano-catalysts. *ACS Appl. Nano Mater.* **2023**, *6* (14), 12805−12815.

(184) Li, H. CO2 capture by various nanoparticles: Recent development and prospective. *Journal of Cleaner Production* **2023**, *414*, No. 137679.

(185) Kumar, T.; Eswari J, S. Review and Perspectives of Emerging Green Technology for the Sequestration of Carbon Dioxide into Value-Added Products: An Intensifying Development. *Energy Fuels* **2023**, *37* (5), 3570−3589.

(186) Xu, S.; Ren, G.; Younis, R. M.; Feng, Q. Revisiting field estimates for carbon dioxide storage in depleted shale gas reservoirs: The role of geomechanics. *International Journal of Greenhouse Gas Control* **2021**, *105*, No. 103222.

(187) Hendriks, C.; Graus, W.; van Bergen, F. *Global carbon dioxide storage potential and costs*; Ecofys: Utrecht, Netherlands, 2004; p *64*.

(188) Bachu, S. Carbon dioxide storage capacity in uneconomic coal beds in Alberta, Canada: Methodology, potential and site identification. *International Journal of Greenhouse Gas Control* **2007**, *1* (3), 374−385.

(189) De Silva, P. N. K.; Ranjith, P. A study of methodologies for CO2 storage capacity estimation of saline aquifers. *Fuel* **2012**, *93*, 13−27.

(190) Thanh, H. V.; Sugai, Y.; Nguele, R.; Sasaki, K. Integrated workflow in 3D geological model construction for evaluation of CO2 storage capacity of a fractured basement reservoir in Cuu Long Basin, Vietnam. *Int. J. Greenhouse Gas Control* **2019**, *90*, No. 102826.

(191) Ajayi, T.; Gomes, J. S.; Bera, A. A review of CO 2 storage in geological formations emphasizing modeling, monitoring and capacity estimation approaches. *Petroleum Science* **2019**, *16*, 1028−1063.

(192) Edwards, R. W.; Celia, M. A.; Bandilla, K. W.; Doster, F.; Kanno, C. M. A model to estimate carbon dioxide injectivity and storage capacity for geological sequestration in shale gas wells. *Environ. Sci. Technol.* **2015**, *49* (15), 9222−9229.

(193) Aminu, M. D.; Nabavi, S. A.; Rochelle, C. A.; Manovic, V. A review of developments in carbon dioxide storage. *Applied Energy* **2017**, *208*, 1389−1419.

(194) Manancourt, A.; Gale, J. A review of capacity estimates for the geological storage of carbon dioxide. *Greenhouse Gas Control Technol.* **2005**, *7*, 2051−2054.

(195) Bachu, S.; Bonijoly, D.; Bradshaw, J.; Burruss, R.; Holloway, S.; Christensen, N. P.; Mathiassen, O. M. CO2 storage capacity estimation: Methodology and gaps. *International Journal of Greenhouse Gas Control* **2007**, *1* (4), 430−443.

https://doi.org/10.1021/acs.energyfuels.3c03004
Energy Fuels XXXX, XXX, XXX−XXX

(196) Kou, Z.; Wang, T.; Chen, Z.; Jiang, J. A fast and reliable methodology to evaluate maximum CO2 storage capacity of depleted coal seams: A case study. *Energy* **2021**, *231*, No. 120992.

(197) Xu, H.; Sang, S.; Yang, J.; Liu, H. CO2 storage capacity of anthracite coal in deep burial depth conditions and its potential uncertainty analysis: a case study of the No. 3 coal seam in the Zhengzhuang Block in Qinshui Basin, China. *Geosciences Journal* **2021**, *25* (5), 715−729.

(198) Day, S.; Duffy, G.; Sakurovs, R.; Weir, S. Effect of coal properties on CO2 sorption capacity under supercritical conditions. *International Journal of Greenhouse Gas Control* **2008**, *2* (3), 342−352.

(199) Han, S.; Sang, S.; Zhang, J.; Xiang, W.; Xu, A. Assessment of CO_2 geological storage capacity based on adsorption isothermal experiments at various temperatures: A case study of No. 3 coal in the Qinshui Basin. *Petroleum* **2023**, *9*, 274.

(200) Sakurovs, R.; Day, S.; Weir, S.; Duffy, G. Application of a modified Dubinin− Radushkevich equation to adsorption of gases by coals under supercritical conditions. *Energy Fuels* **2007**, *21* (2), 992−997.

(201) Godec, M.; Koperna, G.; Gale, J. CO2-ECBM: a review of its status and global potential. *Energy Procedia* **2014**, *63*, 5858−5869.

(202) Anggara, F.; Sasaki, K.; Sugai, Y. The correlation between coal swelling and permeability during CO2 sequestration: A case study using Kushiro low rank coals. *International Journal of Coal Geology* **2016**, *166*, 62−70.

(203) Su, E.; Liang, Y.; Zou, Q.; Niu, F.; Li, L. Analysis of effects of CO2 injection on coalbed permeability: implications for coal seam CO2 sequestration. *Energy Fuels* **2019**, *33* (7), 6606−6615.

(204) Yao, H.; Chen, Y.; Liang, W.; Li, Z.; Song, X. Experimental study on the permeability evolution of coal with CO2 phase transition. *Energy* **2023**, *266*, No. 126531.

(205) Zhang, T.; Zhang, W.; Yang, R.; Liu, Y.; Jafari, M. CO2 capture and storage monitoring based on remote sensing techniques: A review. *Journal of Cleaner Production* **2021**, *281*, No. 124409.

(206) Hill, L. B.; Li, X.; Wei, N. CO2-EOR in China: A comparative review. *International Journal of Greenhouse Gas Control* **2020**, *103*, No. 103173.

(207) Li, J.; Sun, C. Molecular insights on competitive adsorption and enhanced displacement effects of CO2/CH4 in coal for low-carbon energy technologies. *Energy* **2022**, *261*, No. 125176.

(208) Dong, K.; Zhai, Z.; Guo, A. Effects of pore parameters and functional groups in coal on CO2/CH4 adsorption. *ACS omega* **2021**, *6* (48), 32395−32407.

(209) Ye, B.; Jiang, J.; Zhou, Y.; Liu, J.; Wang, K. Technical and economic analysis of amine-based carbon capture and sequestration at coal-fired power plants. *Journal of cleaner production* **2019**, *222*, 476−487.

(210) Zantye, M. S.; Arora, A.; Hasan, M. F. Renewable-integrated flexible carbon capture: A synergistic path forward to clean energy future. *Energy Environ. Sci.* **2021**, *14* (7), 3986−4008.

(211) Fan, C.; Elsworth, D.; Li, S.; Zhou, L.; Yang, Z.; Song, Y. Thermo-hydro-mechanical-chemical couplings controlling CH4 production and CO2 sequestration in enhanced coalbed methane recovery. *Energy* **2019**, *173*, 1054−1077.

(212) Song, Y.; Zou, Q.; Su, E.; Zhang, Y.; Sun, Y. Changes in the microstructure of low-rank coal after supercritical CO2 and water treatment. *Fuel* **2020**, *279*, No. 118493.

(213) Kou, Z.; Wang, H.; Alvarado, V.; McLaughlin, J. F.; Quillinan, S. A. Impact of sub-core scale heterogeneity on CO2/brine multiphase flow for geological carbon storage in the upper Minnelusa sandstones. *Journal of Hydrology* **2021**, *599*, No. 126481.

(214) Zhang, G.; Ranjith, P.; Fu, X.; Li, X. Pore-fracture alteration of different rank coals: Implications for CO2 sequestration in coal. *Fuel* **2021**, *289*, No. 119801.

https://doi.org/10.1021/acs.energyfuels.3c03004
Energy Fuels XXXX, XXX, XXX−XXX